INTERNATIONAL JOURNAL FOR NUMERICAL METHODS IN FLUIDS
Int. J. Numer. Meth. Fluids 2003; **43**:369–406 (DOI: 10.1002/fld.567)

Direct computation of thermodynamic properties of chemically reacting air with consideration to CFD

Joe Iannelli*,†

Department of Mechanical, Aerospace, Biomedical Engineering, The University of Tennessee, 315 Perkins Hall, Knoxville, TN 37996-2030, U.S.A.

SUMMARY

This paper details a two-equation procedure to calculate exactly mass and mole fractions, pressure, temperature, specific heats, speed of sound and the thermodynamic and jacobian partial derivatives of pressure and temperature for a five-species chemically reacting equilibrium air. The procedure generates these thermodynamic properties using as independent variables either pressure and temperature or density and internal energy, for CFD applications. An original element in this procedure consists in the exact physically meaningful solution of the mass-fraction and mass-action equations. Air-equivalent molecular masses for oxygen and nitrogen are then developed to account, within a mixture of only oxygen and nitrogen, for the presence of carbon dioxide, argon and the other noble gases within atmospheric air. The mathematical formulation also introduces a versatile system non-dimensionalization that makes the procedure uniformly applicable to flows ranging from shock-tube flows with zero initial velocity to aerothermodynamic flows with supersonic/hypersonic free-stream Mach numbers. Over a temperature range of more than 10 000 K and pressure and density ranges corresponding to an increase in altitude in standard atmosphere of 30 000 m above sea level, the predicted distributions of mole fractions, constant-volume specific heat, and speed of sound for the model five species agree with independently published results, and all the calculated thermodynamic properties, including their partial derivatives, remain continuous, smooth, and physically meaningful. Copyright © 2003 John Wiley & Sons, Ltd.

KEY WORDS: CFD; thermodynamic properties; equilibrium air

1. INTRODUCTION

The chemical dissociations within reacting air absorb energy and thus lead to lower static temperatures, higher static densities, and different shock-wave positions in comparison to perfect-air predictions. These effects must therefore be modelled accurately for reliable Euler and Navier–Stokes CFD investigation of aerothermodynamic and high-temperature flows.

*Correspondence to: Joe Iannelli, Department of Mechanical, Aerospace, Biomedical Engineering, The University of Tennessee, 315 Perkins Hall, Knoxville, TN 37996-2030, U.S.A.
†E-mail: jiannell@utk.edu

Received September 2000
Revised 19 February 2003

Either curve fits or solutions of the chemical-equilibrium thermodynamics equations can be used to model the thermodynamic properties of reacting equilibrium air. Tannehill and Mugge [1] have used their curve fits for time-dependent CFD calculations. Liou *et al.* [2] used Gordon's and McBride's procedure to generate the equilibrium-air thermodynamic properties and then established curve fit of these properties to simulate numerically high-temperature shock-tube flows. Janicka and Peters [3] selected a similar method in coupling chemical equilibrium with slow chemistry. As another representative example, Prabhu *et al.* [4] and Yee *et al.* [5] used the Srinivasan curve fits for their numerical predictions of inviscid and viscous hypersonic flows. A set of curve fits depends on exponential correlations for the equilibrium constants; hence when improved correlations become available, the curve fits would have to be revised. Furthermore, while many curve fits supply reliable values for pressure, temperature, and other thermodynamic variables, the accuracy of the thermodynamic derivatives of these variables may be insufficient in some curve fits. For several CFD simulations of hypersonic flows, for instance, Yee *et al.* [5], report a degradation in solution accuracy and stability as triggered by discontinuities in the curve-fit thermodynamic derivatives.

As an alternative to curve-fit methods, Park *et al.* [6, 7], and Desideri *et al.* [8] use solutions of classical chemical non-equilibrium and equilibrium thermodynamic systems in their CFD methods and report accurate solutions for several hypersonic blunt body flows. With these systems, the partial derivatives of pressure and temperature can then be analytically determined by differentiating the thermodynamic equations. The results in these references, therefore, bear out the feasibility of coupling at each grid point the solution of a chemical-equilibrium thermodynamic system with Euler and Navier–Stokes CFD algorithms.

This paper presents a computationally efficient solution procedure of an exact thermodynamic model of a five-species, electrically-neutral and chemically reacting air. This model determines 5 species mass fractions, temperature, and pressure via only two equations for nitric-oxide mass fraction and internal energy. The reliability of such reductions have been proven and documented, as also reported by Maas and Pope [9, 10]. What is original in the formulation in this paper is the exact physically meaningful closed-form solution of the mass-fraction and mass-action equations. The model involves an explicit pressure equation of state coupled to a non-linear system of six chemical-equilibrium thermodynamic equations for five mass fractions and temperature. The resulting equations then revert to the familiar perfect-gas expressions in the appropriate temperature and pressure ranges. The developed solution procedure remains valid for any exponential form of the equilibrium constants and, without introducing spurious solutions, succeeds in algebraically reducing this six-equation system to a two-equation system for the nitric-oxide mass fraction and temperature, which are then numerically determined through a rapidly converging Newton's method solution. The remaining mass fractions and then pressure are explicitly calculated using this solution and the thermodynamic and jacobian derivatives of pressure and temperature are exactly determined through an analytical differentiation of the chemical-equilibrium equations in the model.

Classical equilibrium thermodynamics for homogeneous fluids [11–14] shows that any one thermodynamic variable depends on only two other thermodynamic variables. For CFD applications, the selected two thermodynamic variables are density and mass specific internal energy, for these variables are directly available from the continuity and volume-specific total energy equations in the Euler and Navier–Stokes conservation law systems. In the equilibrium thermodynamic system, therefore, density and mass-specific internal energy become assigned

parameters at each grid point. The procedure can also be used with any other two independent thermodynamic variables and the paper presents a method and results that correspond to calculations with pressure and temperature as independent variables.

The neutral air in the procedure encompasses perfect air and consists of a mixture of five non-ionized species: nitric oxide NO and molecular as well as atomic oxygen O_2 and O and nitrogen N_2 and N. Air-equivalent molecular masses are also developed to account for the effect of carbon dioxide, argon, and the other inert noble gases within atmospheric air, without having to involve variable mass fractions of these species within the calculations. The choice of neutral air is justified by the independent results in Reference [12], which confirm that only negligible traces of electrons and hence ionic species exist within equilibrium air for temperatures up to about 9000 K. Each species independently behaves as a perfect-gas for which the familiar perfect-gas law applies. The mixture pressure equation of state is then obtained through Dalton's law as a sum of species partial pressures. The mixture mass-specific internal energy results from the sum of translational and rotational kinetic energies, potential vibrational energy, and formation energy, all at the single equilibrium static temperature. Two additional equations correspond to the conservation of species mass and the mole ratio of oxygen and nitrogen nuclei. The law of mass action provides the completing three equations, which express the equilibrium of any three linearly independent chemical reactions for the five species in equilibrium air. The equilibrium thermodynamic equations are then made non-dimensional by way of a versatile single reference state that makes the procedure uniformly applicable to flows ranging from shock-tube flows with zero initial velocity, to aerothermodynamic flows with supersonic/hypersonic free stream Mach numbers.

Over a temperature range of more than 10 000 K and pressure and density ranges corresponding to an increase in altitude of 30 000 m, slightly greater than 98 000 ft, above sea level, the procedure converges in two or three iterations. Independent published results [12, 14] are available for mole fractions, constant-volume specific heat and speed of sound and the predicted distributions of these variables agree with these published results to the extent that the diagrams for these variables in References [12, 14] virtually coincide with the corresponding figures in this paper. The predicted distributions of pressure and temperature, as well as their partial derivatives, mass fractions, specific heats, and speed of sound remain continuous, smooth and physically meaningful, and the paper details all the thermodynamic and chemical parameters and equations and their partial derivatives for immediate reproduction of the procedure and results.

This paper is organized in 12 Sections. Section 1 presents the governing Euler and Navier–Stokes conservation law systems along with reference thermo-chemical equilibrium pressure equation of state and temperature equation, while Sections 2 develops the chemically-reacting air system of seven algebraic thermochemical equations. These introductory expressions pave the way for the original developments in Sections 3–11. The reference variables and corresponding non-dimensional system are determined in Section 3, while the algebraic and numerical solutions are detailed in Sections 4–5. The analytical determinations of the partial derivatives of pressure and temperature are then presented in Sections 6–7 and Section 8 shows how the developed procedure is used with pressure and temperature as independent variables. Sections 9–10 develop the expressions to calculate the specific heats and speed of sound and Section 11 documents the computational results. Concluding remarks appear in Section 12.

2. NAVIER–STOKES CONSERVATION LAW SYSTEM, PRESSURE EQUATION OF STATE AND TEMPERATURE EQUATION

For arbitrary equilibrium fluids, the multi-dimensional time-dependent governing Navier–Stokes equations in Cartesian conservation law system form is

$$\frac{\partial q}{\partial t} + \frac{\partial f_j(q)}{\partial x_j} = \frac{\partial f_j^v}{\partial x_j} \tag{1}$$

where summation is implied on repeated indices. The Euler equations then originate from (1) by setting the right-hand side identically to zero. In (1), $1 \leqslant j \leqslant n$, where n denotes the number of spatial dimensions, $1 \leqslant n \leqslant 3$, while $\boldsymbol{x} \equiv (x_1, x_2, x_3) \in \Omega \subset \mathrm{Re}^n$ and $t \in [t_o, \infty) \subset \mathrm{Re}$, where Re denotes the field of real numbers and Ω indicates the solution domain.

The state variable q and the inviscid and viscous flux components $f_j(q)$ and f_j^v are defined as

$$q \equiv \begin{Bmatrix} \rho \\ m_1 \\ m_2 \\ m_3 \\ E \end{Bmatrix}, \quad f_j(q) \equiv \begin{Bmatrix} m_j \\ \frac{m_j}{\rho} m_1 + p\delta_j^1 \\ \frac{m_j}{\rho} m_2 + p\delta_j^2 \\ \frac{m_j}{\rho} m_3 + p\delta_j^3 \\ \frac{m_j}{\rho}(E + p) \end{Bmatrix}, \quad f_j^v \equiv \begin{Bmatrix} 0 \\ \tau_{1j} \\ \tau_{2j} \\ \tau_{3j} \\ \sum_{i=1}^{3} \frac{m_i}{\rho} \sigma_{ij} - q_j^{\mathscr{F}} \end{Bmatrix} \tag{2}$$

In q and $f_j(q)$, the dependent variable ρ denotes static density, E indicates the volume-specific total energy, and $m_j = \rho u_j$ corresponds to the jth component of the volume-specific linear momentum $\boldsymbol{m}$, with u_j the corresponding component of the Eulerian velocity. The inviscid flux component $f_j(q)$ then depends on q as well as static pressure p, with δ_j^i, $1 \leqslant i \leqslant n$, defining the Kronecker delta, while the viscous flux component f_j^v depends on u_j as well as the deviatoric stress tensor components $[\tau_{ij}]$ and Fourier heat flux component $q_j^{\mathscr{F}} = -k(T)\partial T/\partial x_j$, in terms of static temperature T, with $k(T)$ indicating thermal conductivity.

For mathematical closure, therefore, the Euler and Navier–Stokes equations require an equation of state (EOS) relating pressure p to the dependent variable q. The Navier–Stokes system must be further augmented with a constitutive relation for $[\tau_{ij}]$, an expression for $k(T)$, and a temperature equation (TE), independent of the EOS, relating T to q. Implicit Euler and Navier–Stokes CFD algorithms additionally require the jacobian partial derivatives of p with respect to q, and an implicit Navier–Stokes CFD also requires the jacobian partial derivatives of T with respect to q.

Functionally cast, the EOS and TE are

$$p = p(q), \qquad T = T(q) \tag{3}$$

For a homogeneous fluid in thermal and chemical equilibrium, thermodynamics stipulates p and T as dependent each upon two other thermodynamic variables [11–14] as

$$p = p(\rho, \varepsilon), \quad T = T(\rho, \varepsilon) \tag{4}$$

where ε denotes the mass-specific internal energy. For a given q, this energy can be obtained from E, which is by definition the sum of volume-specific internal and kinetic energies. As a result,

$$E = \rho\varepsilon + \frac{1}{2\rho}\sum_{i=1}^{n} m_i m_i \Rightarrow \varepsilon = \frac{E}{\rho} - \frac{1}{2\rho^2}\sum_{i=1}^{n} m_i m_i \tag{5}$$

With R and γ respectively denoting the gas constant and ratio of specific heats, the perfect-gas expressions [14] for EOS and TE are

$$p = (\gamma - 1)\rho\varepsilon = (\gamma - 1)\left(E - \frac{1}{2\rho}\sum_{i=1}^{n} m_i m_i\right), \quad T = \frac{p}{R\rho} \tag{6}$$

two well known expressions in CFD.

For a reacting gas, the general expressions that respectively relate pressure p and temperature T to q can be expressed as

$$p = p(\rho, \varepsilon(q)) = p(\rho, \varepsilon(\rho, \boldsymbol{m}, E)), \quad T = T(\rho, \varepsilon(q)) = T(\rho, \varepsilon(\rho, \boldsymbol{m}, E)) \tag{7}$$

which clearly encompass (6). Given q, therefore, p and T as well as their partial derivatives with respect to q are obtained from (7) and the thermodynamics partial derivatives of (7) with respect to ρ and ε. The following sections present and solve the equations that lead to (7) for an electrically neutral mixture of five species.

3. REACTING-AIR EQUATIONS OF STATE

The equations in this section will represent equilibrium, electrically-neutral and chemically-reacting dry air. This type of air encompasses perfect air and consists of a mixture of five non-ionized species: nitric oxide NO and molecular as well as atomic oxygen O_2 and O and nitrogen N_2 and N. In the following, subscript i, $1 \leqslant i \leqslant 5$, indicates the five ordered species O, N, NO, O_2, and N_2. The molecular mass of species i is indicated with M_i. Owing to the species that compose this dry-air model, the species molecular masses satisfy the constraints $M_3 = M_1 + M_2$, $M_4 = 2M_1$, and $M_5 = 2M_2$. Numerical values for these masses are presented in Section 3.4

3.1. Pressure, internal-energy, mass-fraction equations

Each species i independently behaves as a perfect gas with individual EOS

$$p_i = \mathscr{R}T\frac{\rho_i}{M_i} = \mathscr{R}\rho T\frac{\rho_i/\rho}{M_i} = \mathscr{R}\rho T\frac{Y_i}{M_i} \tag{8}$$

where $\mathscr{R}$ and p_i, ρ_i, and Y_i respectively denote the universal gas constant, partial pressure, partial density, and mass fraction of species i. The developments and definition of mole

fraction X_i in Reference [14] yield the result

$$X_i = \frac{\rho_i/M_i}{\rho/M} = \frac{Y_i/M_i}{1/M} = \frac{Y_i/M_i}{\sum_{j=1}^{5} Y_j/M_j}, \quad \frac{1}{M} \equiv \sum_{i=1}^{5} \frac{Y_i}{M_i} \tag{9}$$

which provides each mole fraction in terms of the mass fractions.

For a mixture of perfect species, Dalton's pressure mixing law leads to the mixture pressure equation of state as

$$p = \sum_{i=1}^{5} p_i = \mathscr{R}\rho T \sum_{i=1}^{5} \frac{Y_i}{M_i} = \mathscr{R}\frac{\rho}{M} T \tag{10}$$

The acceptance of Dalton's law thus implies that the mixture EOS has the right-most form indicated in (10).

The mixture mass-specific internal energy ε results from the sum of translational and rotational kinetic energies, potential vibrational energy, and formation energy, all at the equilibrium static temperature T,

$$\varepsilon = T \sum_{i=1}^{5} c_{v_i} Y_i + \sum_{i=3}^{5} \frac{Y_i \mathscr{R}\theta_i^v/M_i}{\exp(\theta_i^v/T) - 1} + \sum_{i=1}^{3} Y_i h_i^0 \tag{11}$$

The second term at the right-hand side of (11) relies upon the rigid-rotor harmonic oscillator model [11–14], which implies the perfect gas equation of state for each species, which in turn is consistent with Dalton's pressure mixing rule. Therefore, the contributions from the ground electronic state are properly modelled for NO, O_2, and N_2. In (11), c_{v_i} denotes the translational/rotational-mode contributions to the ith species constant-volume specific heat, while θ_i^v and h_i^0 are the vibrational temperature and formation enthalpy at 0 K; specific numerical data for these quantities appear in Section 3.4. The constant-volume specific heat c_v then follows from (11) through the derivative $c_v = (\partial\varepsilon/\partial T)_\rho$, as amplified in Section 10. A gas is thermally perfect when M in (10) remains constant, hence in the absence of chemical reactions. A gas is calorically perfect when c_v remains constant, hence in the absence of both chemical reactions and vibrational effects. It is possible for a gas, therefore, to be thermally perfect and calorically not perfect, which happens, for instance, in the absence of chemical reactions when vibrational modes become significant.

A formulation of Equations (10)–(11) in terms of mass fractions simplifies analysis because the expressions for pressure and internal energy are linear with respect to the mass fractions, unlike a formulation in terms of mole fractions. Considering that both ρ and ε are available at each grid point from the conservation law system (1) and (5), Equations (10)–(11) will directly allow the determination of static temperature T and pressure p for the given thermodynamic state (ρ, ε). Fundamental to this determination are the five variable mass fractions Y_i, $1 \leqslant i \leqslant 5$, for which five additional equations are needed.

One equation corresponds to conservation of species mass, which results in the mass-fraction conservation equation

$$\sum_{i=1}^{5} Y_i = 1 \tag{12}$$

Another equation corresponds to the conservation of the mole proportion $\frac{21}{79}$ between oxygen and nitrogen nuclei. In terms of mole fractions, the conservation of this proportion is expressed as $79(X_1 + X_3 + 2X_4) = 21(X_2 + X_3 + 2X_5)$, which corresponds to the following equation in terms of mass fractions

$$\frac{1}{21}\left(\frac{Y_1}{M_1} + \frac{Y_3}{M_3} + 2\frac{Y_4}{M_4}\right) = \frac{1}{79}\left(\frac{Y_2}{M_2} + \frac{Y_3}{M_3} + 2\frac{Y_5}{M_5}\right) \tag{13}$$

The law of mass action provides 3 further equations, which express the equilibrium of any 3 linearly independent chemical reactions for the five species in equilibrium air. The following chemical reactions, two dissociations and one recombination, lead to computationally convenient mass-action equations

$$O_2 \rightleftarrows 2O, \quad N_2 \rightleftarrows 2N, \quad O_2 + N_2 \rightleftarrows 2NO \tag{14}$$

In terms of partial pressures, the mass-action equations for reactions (14) are

$$\frac{p_1^2}{p_4} = k_1(T), \quad \frac{p_2^2}{p_5} = k_2(T), \quad \frac{p_3^2}{p_4 p_5} = k_3(T) \tag{15}$$

and according to statistical thermodynamics [11–14], the partial-pressure equilibrium functions $k_i(T)$ only depend on the static temperature T; the stoichiometric coefficients in (14) then become the exponents in (15). Replacing the partial pressure p_i using (8), yields the mass-fraction law of mass action

$$\frac{Y_1^2}{Y_4} = \frac{M_1^2}{M_4}\frac{k_1(T)}{\mathscr{R}T\rho} = \frac{M_1}{2}\frac{K_1(T)}{\rho} \tag{16}$$

$$\frac{Y_2^2}{Y_5} = \frac{M_2^2}{M_5}\frac{k_2(T)}{\mathscr{R}T\rho} = \frac{M_2}{2}\frac{K_2(T)}{\rho} \tag{17}$$

$$\frac{Y_3^2}{Y_4 Y_5} = \frac{M_3^2}{M_4 M_5}K_3(T) \tag{18}$$

where $K_i(T)$, $1 \leqslant i \leqslant 3$, represent the mass-fraction equilibrium functions, which are traditionally cast as exponential relations [6, 7, 15, 16], as exemplified in Section 3.5. According to the dimensions of terms in (16)–(18), the SI units of $K_1(T)$ and $K_2(T)$ are kg-mol^{-1} kg m^{-3}, whereas $K_3(T)$ remains dimensionless. The following analytical developments will remain valid for any exponential form of these equilibrium functions.

3.2. *Air-equivalent model*

Atmospheric dry air consists of a mixture of oxygen, nitrogen, carbon dioxide, and argon, in addition to traces of other noble gases. The proportions of the chief air constituents are summarized in Table I.

Table I. Composition of atmospheric dry air.

Species		Molecular mass		Mole fraction	Mass fraction
Oxygen	O_2	31.99880	kg kg-mol^{-1}	0.20950	0.231447
Nitrogen	N_2	28.01348	kg kg-mol^{-1}	0.78080	0.755163
Argon	Ar	39.94800	kg kg-mol^{-1}	0.00930	0.012827
Carbon dioxide	CO_2	44.00980	kg kg-mol^{-1}	0.00030	0.000456

Argon and carbon dioxide feature within atmospheric air with seemingly negligible mole fractions, yet their molecular masses are greater than those of oxygen and nitrogen to the extent that they contribute about 0.4% of the total molecular mass of non-reacting atmospheric air M_{air}. This molecular mass is calculated as

$$\begin{aligned} M_{\text{air}} &= \sum_{i=1}^{n_{\text{air}}} X_i M_i = \frac{\mathscr{R}\rho_{\text{sc}} T_{\text{sc}}}{p_{\text{sc}}} = 28.9644827716\ldots \text{ kg kg-mol}^{-1} \\ \rho_{\text{sc}} &= 1.225 \text{ kg m}^{-3}, \quad T_{\text{sc}} = 288.15 \text{ K}, \quad p_{\text{sc}} = 101,325.024 \text{ Pa} \end{aligned} \tag{19}$$

where n_{air} denotes the total number of atmospheric air species, and ρ_{sc}, p_{sc} and T_{sc} denote standard-condition density, temperature, and pressure.

Reported calculations of high-temperature air flows, [6–8, 14], model air as a mixture of oxygen, nitrogen, and nitric oxide, in their various forms. In non-reacting conditions, the mole fractions of oxygen and nitrogen in this mixture respectively become 0.21 and 0.79; this model, therefore, accepts the presence of 1.18% more nitrogen moles than there are within atmospheric air. The determination of pressure, temperature or density from the perfect gas law (10) with these mole fractions approximate the corresponding data of standard atmosphere with an error of about 0.4%.

In atmospheric air, carbon dioxide is present in minute amounts in comparison to oxygen and nitrogen, while argon and the other noble gases in air remain inert towards all other elements and chemicals [15]. The essential effect of carbon dioxide, argon and the other noble gases in air, therefore, is to catalyze the chemical reactions of oxygen and nitrogen through collisions and make air heavier than a mixture of only oxygen and nitrogen, reacting or not. This situation is mathematically reflected in the following pressure and internal energy equations, expressed similarly to (10) and (11), but in terms of mole fractions from (9) and accounting for all inert air species

$$\begin{aligned} p &= \frac{\mathscr{R}\rho T}{\sum_{j=1}^{5} X_j M_j + M_{\text{oth}}}, \quad \varepsilon = T\left(\frac{\sum_{i=1}^{5} \bar{c}_i}{\sum_{j=1}^{5} X_j M_j + M_{\text{oth}}} + c_{v_{\text{oth}}}\right) \\ &\quad + \sum_{i=3}^{5} \frac{\mathscr{R}\theta_i^v X_i}{(\exp(\theta_i^v/T) - 1)\left(\sum_{j=1}^{5} X_j M_j + M_{\text{oth}}\right)} + \sum_{i=1}^{3} \frac{\mathscr{R}\bar{h}_i X_i}{\sum_{j=1}^{5} X_j M_j + M_{\text{oth}}} \end{aligned} \tag{20}$$

Table II. Errors induced by the $\frac{21}{79}$ mole ratio.

Variable	Non air-equivalent	Air-equivalent
$X_{4,1}$	0.24%	0.24%
$X_{5,2}$	1.18%	1.18%
$Y_{4,1}$	0.64%	1.36%
$Y_{5,2}$	1.58%	1.36%
M_{air}	−0.39%	0.00%
R	0.39%	0.00%
$c_{v_{\text{air}}}$	0.39%	0.00%
$c_{p_{\text{air}}}$	0.39%	0.00%
γ	0.00%	0.00%

where $\bar{c}_i$, $\bar{h}_i$, $c_{v_{\text{oth}}}$, and M_{oth} respectively denote the constant coefficients within c_{v_i} and h_i^0, detailed in Section 3.4, and the contribution to the translation/rotational specific heat and molecular mass of the other species besides nitric oxide and atomic and molecular oxygen and nitrogen. The effect of the presence of other chemicals within air, besides oxygen and nitrogen, can therefore be modelled by establishing air-equivalent molecular masses for oxygen and nitrogen so that the molecular mass of a non-reacting mixture with mole ratio $\frac{21}{79}$ of these two species equals the molecular mass of non-reacting air, hence

$$0.21M_4 + 0.79M_5 = M_{\text{air}} \tag{21}$$

where M_4 and M_5 respectively denote the air-equivalent molecular masses of oxygen and nitrogen. The second constraint to determine both M_4 and M_5 is chosen to be preservation of the mass-fraction ratio

$$\frac{Y_5^{\text{air}}}{Y_4^{\text{air}}} = \frac{Y_5}{Y_4} = \frac{X_5 M_5}{X_4 M_4} = \frac{0.79M_5}{0.21M_4} = 3.26279010234 \tag{22}$$

where Y_4^{air} and Y_5^{air} are listed in Table I. The errors induced by the $\frac{21}{79}$ mole ratio are summarized in Table II for both non-equivalent and equivalent masses, where R, $c_{v_{\text{air}}}$, $c_{p_{\text{air}}}$ and γ respectively denote the specific, not universal, gas constant, constant-volume and constant-pressure specific heats of non-reacting air, and specific heat ratio.

With the air-equivalent masses M_4 and M_5, Equations (10), (11) for non-reacting conditions exactly yields the pressure and temperature of non-reacting atmospheric air.

3.3. Non-dimensional reacting-air equations of state

The system of Equations (10)–(11) and (16)–(18) are made non-dimensional by way of a versatile single reference state that makes this system uniformly applicable to conditions ranging from flows with a specified fixed initial state with zero velocity, typical of shock-tube flows, to flows with an identifiable free stream state, typical of supersonic/hypersonic aerothermodynamic flows.

For an available free stream state with representative constant density ρ_∞, pressure p_∞, temperature T_∞, and Mach number M_∞, the reference molecular mass, density, mass-specific energy (speed squared), pressure and temperature are expressed as

$$M_r = \frac{\mathscr{R}\rho_\infty T_\infty}{p_\infty}$$

$$\rho_r = \rho_\infty$$

$$U_r^2 = U_\infty^2 = \gamma_\infty M_\infty^2 (\mathscr{R}/M_r) T_\infty, \quad \gamma_\infty \equiv \frac{c_\infty^2}{p_\infty/\rho_\infty} \tag{23}$$

$$p_r = \rho_r U_r^2 = \gamma_\infty M_\infty^2 p_\infty$$

$$T_r = \frac{p_r}{\rho_r(\mathscr{R}/M_r)} = \frac{U_r^2}{(\mathscr{R}/M_r)} = \gamma_\infty M_\infty^2 T_\infty \tag{24}$$

where c_∞^2 denotes the square of the free-stream speed of sound. When the free-stream air behaves as a standard-condition perfect air, then $\gamma_\infty = \frac{7}{5}$ and when ρ_∞, p_∞ and T_∞ already satisfy the perfect-gas law, then the reference molecular mass M_r corresponds to the air molecular mass. Otherwise it simply represents a scaling factor by which to divide the species molecular masses.

For a typical shock-tube initial state with representative constant pressure p_∞, temperature T_∞, and density ρ_∞ the reference variables are

$$M_r = \frac{\mathscr{R}\rho_\infty T_\infty}{p_\infty}$$

$$\rho_r = \rho_\infty$$

$$U_r^2 = (\mathscr{R}/M_r) T_\infty = \gamma_\infty M_\infty^2 (\mathscr{R}/M_r) T_\infty, \quad M_\infty^2 \equiv \frac{1}{\gamma_\infty} \tag{25}$$

$$p_r = p_\infty = \gamma_\infty M_\infty^2 p_\infty$$

$$T_r = T_\infty = \gamma_\infty M_\infty^2 T_\infty \tag{26}$$

where γ_∞ is calculated as in (23). Heed that for $M_\infty^2 = 1/\gamma_\infty$, this reference state formally coincides with (23)–(24). Therefore, by setting M_∞ equal to either the free-stream Mach number or $1/\gamma_\infty$, depending on the flow class, a unique set of non-dimensional equations of state emerges for both reference sets (23)–(24) and (25)–(26).

With definitions (23)–(24) and (25)–(26), the reference pressure, density, and temperature then satisfy the perfect gas law. For high Mach numbers they constitute sizable constants that conveniently scale down the large pressure, density and temperature across a normal shock, like the stagnation-streamline normal section of supersonic and hypersonic aerodynamic-flow bow shocks.

Using either the reference states (23)–(24) or (25)–(26), the non-dimensional density, mass-specific internal energy, pressure and temperature are then expressed as

$$\begin{aligned} \tilde{\rho} &= \frac{\rho}{\rho_r}, \quad \tilde{\varepsilon} = \frac{\varepsilon}{U_r^2} = \frac{\varepsilon}{\gamma_\infty M_\infty^2 (\mathscr{R}/M_r) T_\infty} \\ \tilde{p} &= \frac{p}{p_r} = \frac{p}{\gamma_\infty M_\infty^2 p_\infty}, \quad \tilde{T} = \frac{T}{T_r} = \frac{T}{\gamma_\infty M_\infty^2 T_\infty} \end{aligned} \tag{27}$$

The corresponding non-dimensional pressure equation is

$$\tilde{p} = \frac{\mathscr{R}\tilde{\rho}\rho_r \tilde{T} T_r}{p_r} \sum_{i=1}^{5} \frac{Y_i}{M_i} = \frac{\mathscr{R}\tilde{\rho}\tilde{T}}{(\mathscr{R}/M_r)} \sum_{i=1}^{5} \frac{Y_i}{M_i} = \tilde{\rho}\tilde{T} \sum_{i=1}^{5} \frac{Y_i}{(M_i/M_r)} = \tilde{\rho}\tilde{T} \sum_{i=1}^{5} \frac{Y_i}{\tilde{M}_i} \tag{28}$$

where $\widetilde{M_i} = M_i/M_r$. It follows that with this non-dimensionalization, the universal gas constant $\mathscr{R}$ no longer appears in this non-dimensional equation of state. The non-dimensional energy equation is

$$\begin{aligned} \tilde{\varepsilon} = {} & \frac{T}{\gamma_\infty M_\infty^2 (\mathscr{R}/M_r) T_\infty} \sum_{i=1}^{5} c_{v_i} Y_i + \sum_{i=3}^{5} \frac{Y_i \mathscr{R} \theta_i^v / M_i}{(\gamma_\infty M_\infty^2 (\mathscr{R}/M_r) T_\infty) \cdot (\exp(\theta_i^v/T) - 1)} \\ & + \sum_{i=1}^{3} Y_i \frac{h_i^0}{\gamma_\infty M_\infty^2 (\mathscr{R}/M_r) T_\infty} \end{aligned} \tag{29}$$

which becomes

$$\tilde{\varepsilon} = \frac{T}{\gamma_\infty M_\infty^2 T_\infty} \sum_{i=1}^{5} \left(c_{v_i} \frac{M_r}{\mathscr{R}} \right) Y_i + \sum_{i=3}^{5} \frac{Y_i \left(\dfrac{\theta_i^v}{\gamma_\infty M_\infty^2 T_\infty} \right) \dfrac{1}{M_i/M_r}}{\exp\left(\left(\dfrac{\theta_i^v}{\gamma_\infty M_\infty^2 T_\infty} \right) \dfrac{\gamma_\infty M_\infty^2 T_\infty}{T} \right) - 1} + \sum_{i=1}^{3} Y_i \tilde{h}_i^0 \tag{30}$$

and is simplified as

$$\tilde{\varepsilon} = \tilde{T} \sum_{i=1}^{5} \tilde{c}_{v_i} Y_i + \sum_{i=3}^{5} \frac{Y_i \tilde{\theta}_i^v / \tilde{M}_i}{\exp(\tilde{\theta}_i^v / \tilde{T}) - 1} + \sum_{i=1}^{3} Y_i \tilde{h}_i^0 \tag{31}$$

and the universal gas constant $\mathscr{R}$ no longer multiplies any term in this equation. Furthermore, as indicated in Section 3.4, the magnitudes of the non-dimensional specific heat $\tilde{c}_{v_i}$, characteristic vibrational temperature $\tilde{\theta}_i^v$, and formation enthalpy $\tilde{h}_i^0$ decrease with respect to their dimensional values.

Since the mass fractions Y_i are already dimensionless variables, the non-dimensional species conservation equations are

$$\sum_{i=1}^{5} Y_i = 1, \quad \frac{1}{21} \left(\frac{Y_1}{\tilde{M}_1} + \frac{Y_3}{\tilde{M}_3} + 2\frac{Y_4}{\tilde{M}_4} \right) = \frac{1}{79} \left(\frac{Y_2}{\tilde{M}_2} + \frac{Y_3}{\tilde{M}_3} + 2\frac{Y_5}{\tilde{M}_5} \right) \tag{32}$$

The non-dimensional mass-action equations are then

$$\frac{Y_1^2}{Y_4} = \frac{\tilde{M}_1}{2}\frac{K_1(\tilde{T})}{\tilde{\rho}(\rho_r/M_r)} = \frac{\tilde{M}_1}{2}\frac{\tilde{K}_1(\tilde{T})}{\tilde{\rho}}, \quad \tilde{K}_1(\tilde{T}) \equiv \frac{K_1(\tilde{T})}{\rho_r/M_r} \tag{33}$$

$$\frac{Y_2^2}{Y_5} = \frac{\tilde{M}_2}{2}\frac{K_2(\tilde{T})}{\tilde{\rho}(\rho_r/M_r)} = \frac{\tilde{M}_2}{2}\frac{\tilde{K}_2(\tilde{T})}{\tilde{\rho}}, \quad \tilde{K}_2(\tilde{T}) \equiv \frac{K_2(\tilde{T})}{\rho_r/M_r} \tag{34}$$

$$\frac{Y_3^2}{Y_4 Y_5} = \frac{\tilde{M}_3^2}{\tilde{M}_4\tilde{M}_5}\tilde{K}_3(\tilde{T}) \tag{35}$$

where $\tilde{K}_i$, $1 \leqslant i \leqslant 3$, denote the non-dimensional equilibrium functions, as exemplified in Section 3.5.

3.4. Chemical and thermodynamics parameters

In the units of kg kg-mol^{-1}, the molecular masses for the chosen five species are [16]

$$\begin{gathered} M_1^{na} = 15.99940, \quad M_2^{na} = 14.00674 \\ M_3^{na} = 30.00614, \quad M_4^{na} = 31.99880, \quad M_5^{na} = 28.01348 \end{gathered} \tag{36}$$

where superscript '*na*' signifies non air-equivalent masses. In the same units, the corresponding air-equivalent masses are

$$\begin{gathered} M_1 = 16.17791, \quad M_2 = 14.03149 \\ M_3 = 30.20940, \quad M_4 = 32.35582, \quad M_5 = 28.06298 \end{gathered} \tag{37}$$

Both non-equivalent and equivalent masses satisfy the constraints $M_3 = M_1 + M_2$, $M_4 = 2M_1$, and $M_5 = 2M_2$.

In SI units, the universal gas constant is

$$\mathscr{R} = 8,314.34 \text{ J kg-mol}^{-1} \text{ K}^{-1} \tag{38}$$

For the selected five species, the vibrational temperatures in (11) are expressed as [13]

$$\theta_3^v = 2,740 \text{ K}, \quad \theta_4^v = 2,270 \text{ K}, \quad \theta_5^v = 3,390 \text{ K} \tag{39}$$

and the formation enthalpies result from Reference [17] as

$$h_1^0 = 29,682.446\frac{\mathscr{R}}{M_1} \text{ J kg}^{-1}, \quad h_2^0 = 56,627.830\frac{\mathscr{R}}{M_2} \text{ J kg}^{-1}, \quad h_3^0 = 10,797.780\frac{\mathscr{R}}{M_3} \text{ J kg}^{-1} \tag{40}$$

Further, each c_{v_i} in (11) is determined as [11–14, 17]

$$\begin{gathered} c_{v_1} = \frac{3}{2}\frac{\mathscr{R}}{M_1} \text{ J kg}^{-1} \text{ K}^{-1}, \quad c_{v_2} = \frac{3}{2}\frac{\mathscr{R}}{M_2} \text{ J kg}^{-1} \text{ K}^{-1} \\ c_{v_3} = \frac{5}{2}\frac{\mathscr{R}}{M_3} \text{ J kg}^{-1} \text{ K}^{-1}, \quad c_{v_4} = \frac{5}{2}\frac{\mathscr{R}}{M_4} \text{ J kg}^{-1} \text{ K}^{-1}, \quad c_{v_5} = \frac{5}{2}\frac{\mathscr{R}}{M_5} \text{J kg}^{-1} \text{ K}^{-1} \end{gathered} \tag{41}$$

These expressions result from the kinetic theory of gases [11, 13, 14] dictating that a monoatomic gas, like O, possesses three independent energy absorption mechanisms (degrees of freedom), which correspond to the translation kinetic energy of the motion along three mutually perpendicular directions; a diatomic gas, like N_2, has five such degrees, three of translation and two of rotation about two mutually perpendicular axes that are orthogonal to the axis through the molecule nuclei.

The non-dimensional form of the internal energy equations (31) thus originates from the following expressions

$$\tilde{c}_{v_1} = \frac{3}{2}\frac{1}{\tilde{M}_1}, \quad \tilde{c}_{v_2} = \frac{3}{2}\frac{1}{\tilde{M}_2}, \quad \tilde{c}_{v_3} = \frac{5}{2}\frac{1}{\tilde{M}_3}, \quad \tilde{c}_{v_4} = \frac{5}{2}\frac{1}{\tilde{M}_4}, \quad \tilde{c}_{v_5} = \frac{5}{2}\frac{1}{\tilde{M}_5} \tag{42}$$

for each specific heat,

$$\tilde{\theta}_3^v = \frac{2,740}{\gamma_\infty M_\infty^2 T_\infty}, \quad \tilde{\theta}_4^v = \frac{2,270}{\gamma_\infty M_\infty^2 T_\infty}, \quad \tilde{\theta}_5^v = \frac{3,390}{\gamma_\infty M_\infty^2 T_\infty} \tag{43}$$

for each vibrational temperature, and

$$\tilde{h}_1^0 = \frac{29,682.446}{\gamma_\infty M_\infty^2 T_\infty \tilde{M}_1}, \quad \tilde{h}_2^0 = \frac{56,627.830}{\gamma_\infty M_\infty^2 T_\infty \tilde{M}_2}, \quad \tilde{h}_3^0 = \frac{10,797.780}{\gamma_\infty M_\infty^2 T_\infty \tilde{M}_3} \tag{44}$$

for each formation enthalpy, which collectively indicate that either (23)–(24) or (25)–(26) can significantly scale down these parameters.

3.5. Chemical equilibrium functions

While the procedure developed to solve system (28), (31)–(35) is valid for any exponential form of equilibrium functions $K_i(T)$, $i = 1, 2, 3$, the numerical results presented in Section 12 were generated using the specific expressions of $K_i(T)$ reported in Reference [17]. These expressions are

$$K_i(T) = \exp(A_{i4}Z^4 + A_{i3}Z^3 + A_{i2}Z^2 + A_{i1}Z + A_{i0}), \quad Z \equiv \log\left(\frac{10\,000}{T}\right) \tag{45}$$

where A_{ij} denote constant coefficients that also ensure a smooth asymptotic convergence of the equilibrium-air system (28), (31)–(35) to either a standard-condition perfect gas equation of state, at lower temperatures, or a high-temperature equation of state, at higher temperatures.

According to (16)–(18), this asymptotic convergence is achieved when $K_i(T)$, $i = 1, 2, 3$, approach zero at lower temperatures, since Y_1, Y_2, and Y_3 vanish in this temperature range. Furthermore, $K_1(T)$ and $K_2(T)$ have to increase monotonically at higher temperatures, since Y_4 and Y_5 vanish at these temperatures. Conversely, $K_3(T)$ has to remain bounded at higher temperatures as a sufficient condition for attaining from (18) a vanishing Y_3. The corresponding coefficients A_{ij} for these equilibrium functions are given in Table III.

Heed that the coefficients A_{i0}, $i = 1, 2$, in Table III result by adding log(1000) to those in [17], which corresponds to a change of units from mol cm^{-3} to kg-mol m^{-3}. The equilibrium functions in (45) are compactly expressed as

$$K_i(T) = \exp(G_i(T)) \tag{46}$$

Table III. Coefficients for equilibrium functions (45).

i	A_{i4}	A_{i3}	A_{i2}	A_{i1}	A_{i0}
1	−0.466031	−1.78672	−1.24877	−5.15926	+2.97975
2	−1.007340	−2.74128	−2.93912	−11.0496	−2.06856
3	−0.196317	−0.42724	−0.86667	−1.65356	+0.61473

Consequently, the derivative of $K_i(T)$ with respect to T is cast as

$$\frac{\mathrm{d}K_i(T)}{\mathrm{d}T} = \exp(G_i(T))\frac{\mathrm{d}G_i(T)}{\mathrm{d}T} = K_i\frac{\mathrm{d}G_i}{\mathrm{d}T} \tag{47}$$

Expressions (33)–(34) feature the non-dimensional equilibrium functions $\tilde{K}_i(\tilde{T})$ corresponding to (45). These non-dimensional equilibrium functions depend upon $\tilde{T}$ by expressing the variable Z in (45) as

$$Z = \frac{10\,000}{T} = \left(\frac{10\,000}{\gamma_\infty M_\infty^2 T_\infty}\right)\left(\frac{\gamma_\infty M_\infty^2 T_\infty}{T}\right) = \frac{\bar{T}}{\tilde{T}}, \quad \bar{T} = \frac{10\,000}{\gamma_\infty M_\infty^2 T_\infty} \tag{48}$$

where $\bar{T}$ can be made substantially smaller than 10 000.

4. ALGEBRAIC SOLUTION

One original contribution of this paper is the exact algebraic reduction of the system of six non-linear equations to two non-linear equations. This result follows from having determined the exact physically meaningful closed-form solution of the mass-action and mass-fraction equations.

Dropping the tildes for simplicity, yet remembering that all variables in the following expressions are non-dimensional ones, the non-dimensional equations of state are

$$p = \rho T\sum_{i=1}^{5}\frac{Y_i}{M_i} \tag{49}$$

$$\varepsilon = T\sum_{i=1}^{5}c_{v_i}Y_i + \sum_{i=3}^{5}\frac{Y_i\theta_i^v/M_i}{\exp(\theta_i^v/T)-1} + \sum_{i=1}^{3}Y_i h_i^0 \tag{50}$$

$$\sum_{i=1}^{5}Y_i = 1 \tag{51}$$

$$\frac{1}{21}\left(\frac{Y_1}{M_1}+\frac{Y_3}{M_3}+2\frac{Y_4}{M_4}\right) = \frac{1}{79}\left(\frac{Y_2}{M_2}+\frac{Y_3}{M_3}+2\frac{Y_5}{M_5}\right) \tag{52}$$

$$\frac{Y_1^2}{Y_4} = \frac{M_1}{2}\frac{K_1(T)}{\rho} \tag{53}$$

$$\frac{Y_2^2}{Y_5} = \frac{M_2}{2}\frac{K_2(T)}{\rho} \tag{54}$$

$$\frac{Y_3^2}{Y_4 Y_5} = \frac{M_3^2}{M_4 M_5} K_3(T) \tag{55}$$

The five mass fractions Y_i, $1 \leqslant i \leqslant 5$ and static temperature T can then be theoretically obtained by solving the non-linear system of the last six equations given above and practically determined through a numerical iterative procedure, which for CFD applications can become a daunting proposition if such a 6×6 system required even a few iterations at each of hundreds of thousands of grid points. In the following developments, however, the four variable mass fractions Y_i, $i = 1, 2, 4, 5$, of the six variables in this 6×6 system are explicitly expressed algebraically in terms of only two variables: nitric-oxide mass fraction Y_3 and temperature T. The complete solution of system (49)–(55) is then obtained from the solution for these two variables of a far less daunting 2×2 system. The selection of the specific relations leading to this system was predicated on the elimination of the non-physical spurious solutions that can solve a non-linear algebraic system of equations. This criterion ensured that the resulting equations only possess a physically meaningful solution.

The two mass fractions Y_1 and Y_2 in the two linear equations (51)–(52) can be explicitly solved in terms of Y_3, Y_4, and Y_5. The expression for Y_1 results by summing (52) to the product of (51) and $1/(79M_2)$; Y_2 then follows from (51). This sequence of operations yields the expressions

$$Y_1 = \frac{0.21M_1}{0.21M_1 + 0.79M_2} - \frac{M_1}{M_3} Y_3 - Y_4 \tag{56}$$

$$Y_2 = \frac{0.79M_2}{0.21M_1 + 0.79M_2} - \frac{M_2}{M_3} Y_3 - Y_5 \tag{57}$$

For conciseness, these two expressions are then cast as

$$Y_1 = \alpha_{10} - \alpha_{13} Y_3 - Y_4 \tag{58}$$

$$Y_2 = \alpha_{20} - \alpha_{23} Y_3 - Y_5 \tag{59}$$

where the constants α_{10}, α_{13}, α_{20}, and α_{23} follow from inspection of (56)–(57).

The explicit relations for Y_4 and Y_5 result from inserting (58) and (59) into (53) and (54) respectively. This operation yields the quadratic equations

$$Y_4^2 - 2\left(\alpha_{10} - \alpha_{13} Y_3 + \frac{M_1}{2} \frac{K_1(T)}{2\rho}\right) Y_4 + (\alpha_{10} - \alpha_{13} Y_3)^2 = 0 \tag{60}$$

$$Y_5^2 - 2\left(\alpha_{20} - \alpha_{23} Y_3 + \frac{M_2}{2} \frac{K_2(T)}{2\rho}\right) Y_5 + (\alpha_{20} - \alpha_{23} Y_3)^2 = 0 \tag{61}$$

which remain valid for any form of the equilibrium function $K_i(T)$, $i = 1, 2$, and intrinsically depend upon Y_3. Of the two mathematical solutions for each of (60) and (61), the solution

devoid of physical significance is discarded and the physically meaningful solutions are then established as

$$Y_4 = \alpha_{10} - \alpha_{13} Y_3 + \frac{M_1}{2}\frac{K_1(T)}{2\rho} - \left(\frac{M_1}{2}\frac{K_1(T)}{\rho}\left(\alpha_{10} - \alpha_{13} Y_3 + \frac{M_1}{2}\frac{K_1(T)}{4\rho}\right)\right)^{1/2} \tag{62}$$

$$Y_5 = \alpha_{20} - \alpha_{23} Y_3 + \frac{M_2}{2}\frac{K_2(T)}{2\rho} - \left(\frac{M_2}{2}\frac{K_2(T)}{\rho}\left(\alpha_{20} - \alpha_{23} Y_3 + \frac{M_2}{2}\frac{K_2(T)}{4\rho}\right)\right)^{1/2} \tag{63}$$

According to the algebraic sign of the coefficients in (62)–(63), Y_4 and Y_5 are positive if so are the expressions $\alpha_{i0} - \alpha_{i3} Y_{13}$, $i = 1,2$, since K_1 and K_2 are intrinsically positive. Given the definition of the coefficients α_{10}, α_{13}, α_{20}, α_{23} in (58)–(59), this condition is always met since Y_3 stays below one. For increasing temperature, furthermore, both Y_4 and Y_5 from (62)–(63) consistently approach zero, as physically correct, owing to the monotonic increase of K_1 and K_2. Finally, at lower temperatures, K_1, K_2 and Y_3 approach zero. Hence, Y_4 and Y_5 from (62)–(63) converge to their respective perfect-gas numerical values, while from (56)–(57) both Y_1 and Y_2 vanish.

By virtue of (62)–(63), Y_4 and Y_5 are functionally expressed as

$$Y_4 = Y_4(Y_3(\rho,\varepsilon), T(\rho,\varepsilon), \rho), \quad Y_5 = Y_5(Y_3(\rho,\varepsilon), T(\rho,\varepsilon), \rho) \tag{64}$$

and the functional relations for Y_1 and Y_2 from (56)–(57) are then

$$Y_1 = Y_1(Y_3(\rho,\varepsilon), Y_4(Y_3(\rho,\varepsilon), T(\rho,\varepsilon), \rho)), \quad Y_2 = Y_2(Y_3(\rho,\varepsilon), Y_5(Y_3(\rho,\varepsilon), T(\rho,\varepsilon), \rho)) \tag{65}$$

which show that these four mass fractions explicitly depend upon ρ and ε as well as Y_3 and T. For the thermodynamic state (ρ,ε), existing at each grid node from (5) and the continuity and energy conservation equations in (1), and associated Y_3 and T, therefore, both Y_4 and Y_5 are directly obtained from (62)–(63), which then allows determining both Y_1 and Y_2 from (56)–(57). The corresponding pressure is then determined from (49). A complete solution for the non-linear 6-equation system (50)–(55), is thus obtained when both Y_3 and T are determined.

5. CALCULATION OF Y_3 AND T

The two equations that remain to be solved for system (50)–(55) are the nitric-oxide mass-action equation (55) and the mass-specific internal energy equation (50). The solution for T and Y_3 is thus determined by solving the two-equation system

$$f_1(\rho, Y_3, T) \equiv Y_3 - M_3\left(\frac{Y_4}{M_4}\frac{Y_5}{M_5}K_3(T)\right)^{1/2} = 0 \tag{66}$$

$$f_2(\rho, \varepsilon, Y_3, T) \equiv \varepsilon - T\sum_{i=1}^{5} c_{v_i} Y_i - \sum_{i=3}^{5}\frac{Y_i \theta_i^v / M_i}{\exp(\theta_i^v/T) - 1} - \sum_{i=1}^{3} Y_i h_i^0 = 0 \tag{67}$$

with Y_i, $i = 1,2,4,5$ expressed via (58)–(59) and (62)–(63). For a positive thermodynamic state (ρ,ε), each term in (66)–(67), is a non-positive monotone function of temperature T

and nitric oxide mass fraction Y_3. Furthermore, the square root expression in (66) is also a non-negative monotone function of T. Therefore, a solution of system (66)–(67) with positive Y_3 and T exists and is unique. This solution is numerically determined by solving this system through Newton's method

5.1. Numerical solution

In system (66)–(67), the thermodynamic state (ρ, ε) is known and fixed at each grid point. For the auxiliary variable $Q \equiv \{Y_3, T\}^{\mathrm{T}}$, therefore, this system is cast as

$$F(\rho, \varepsilon, Q) \equiv F(\rho, \varepsilon, Y_3, T) \equiv \left\{ \begin{array}{c} f_1(\rho, Y_3, T) \\ f_2(\rho, \varepsilon, Y_3, T) \end{array} \right\} = 0 \tag{68}$$

The Newton's algorithm to solve this system is

$$Q^{i+1} = Q^i - \left[\left(\frac{\partial F}{\partial Q} \right)_{\rho, \varepsilon}^{i} \right]^{-1} \{F^s\} \tag{69}$$

where superscript i denotes the iteration index. The initial estimate Q^0 at a grid node can coincide with the value of Q at an adjacent grid point where this system has already been solved. If no solution for Q is available at an adjacent node, as is typical when (66)–(67) is solved at the first grid node, then an initial estimate for Q^0 can correspond to low T and consequently $Y_3 \equiv 0$. These two selections are consistent with each other because K_3, Y_1 and Y_2 approach zero at lower temperatures, which leads to a vanishing Y_3, as a solution of (66). Under the same low-temperature conditions, Equation (67) then asymptotically converges to the corresponding perfect gas expressions. With symmetrized f_1 and f_2 with respect to the f axis, that is $f_1(-Y_3, -T) = f_1(Y_3, T)$ and $f_2(-Y_3, -T) = f_2(Y_3, T)$, the absolute value of both Y_3^i and T^i, at the end of each iteration, will equally lead to the solution of (66)–(67), as also indicated in Reference [18] for a hydrocarbon equilibrium thermodynamic system. Iteration (69) is cast in closed form, since the 2×2 Jacobian is analytically determined in the following section. Hence, evaluating (69) is relatively inexpensive, leads to a quadratically convergent process, and directly yields Y_3 and T.

5.2. Iteration partial derivatives

For a given flow state $q \equiv \{\rho, \boldsymbol{m}, E\}^{\mathrm{T}}$, and hence for a fixed (ρ, ε), Equations (66)–(67) are functionally cast as

$$f_1(Y_3, Y_4(Y_3, T), Y_5(Y_3, T,), T) = 0 \tag{70}$$

$$f_2(T, Y_1(Y_3, Y_4(Y_3, T,)), Y_2(Y_3, Y_5(Y_3, T,)), Y_3, Y_4(Y_3, T,), Y_5(Y_3, T)) = 0 \tag{71}$$

Therefore, the partial derivatives in the jacobian matrix in (69) are expressed as

$$\left[\left(\frac{\partial F}{\partial Q} \right)_q \right] \equiv \left[\begin{array}{cc} \left(\dfrac{\partial f_1}{\partial Y_3} \right)_{q,T}, & \left(\dfrac{\partial f_1}{\partial T} \right)_{q, Y_3} \\ \left(\dfrac{\partial f_2}{\partial Y_3} \right)_{q,T}, & \left(\dfrac{\partial f_2}{\partial T} \right)_{q, Y_3} \end{array} \right] \tag{72}$$

where subscripts denote the variables held constant in the partial differentiation. The partial derivatives in (72) are thus determined by application of the chain rule to (66)–(67), which yields the unabridged forms

$$\left(\frac{\partial f_1}{\partial Y_3}\right)_{q,T} = \left(\frac{\partial f_1}{\partial Y_3}\right)_{q,Y_4,Y_5,T} + \left(\frac{\partial f_1}{\partial Y_4}\right)_{q,Y_3,Y_5,T} \cdot \left(\frac{\partial Y_4}{\partial Y_3}\right)_{q,T} + \left(\frac{\partial f_1}{\partial Y_5}\right)_{q,Y_3,Y_4,T} \cdot \left(\frac{\partial Y_5}{\partial Y_3}\right)_{q,T} \tag{73}$$

$$\left(\frac{\partial f_1}{\partial T}\right)_{q,Y_3} = \left(\frac{\partial f_1}{\partial T}\right)_{q,Y_4,Y_5,Y_3} + \left(\frac{\partial f_1}{\partial Y_4}\right)_{q,Y_3,Y_5,T} \cdot \left(\frac{\partial Y_4}{\partial T}\right)_{q,Y_3} + \left(\frac{\partial f_1}{\partial Y_5}\right)_{q,Y_3,Y_4,T} \cdot \left(\frac{\partial Y_5}{\partial T}\right)_{q,Y_3} \tag{74}$$

$$\left(\frac{\partial f_2}{\partial Y_3}\right)_{q,T} = \left(\frac{\partial f_2}{\partial Y_3}\right)_{q,Y_1,Y_2,Y_4,Y_5,T} + \left(\frac{\partial f_2}{\partial Y_1}\right)_{q,Y_2,Y_3,Y_4,Y_5,T} \cdot \left(\frac{\partial Y_1}{\partial Y_3}\right)_{q,T} + \left(\frac{\partial f_2}{\partial Y_2}\right)_{q,Y_1,Y_3,Y_4,Y_5,T} \cdot \left(\frac{\partial Y_2}{\partial Y_3}\right)_{q,T} + \left(\frac{\partial f_2}{\partial Y_4}\right)_{q,Y_1,Y_2,Y_3,Y_5,T} \cdot \left(\frac{\partial Y_4}{\partial Y_3}\right)_{q,T} + \left(\frac{\partial f_2}{\partial Y_5}\right)_{q,Y_1,Y_2,Y_3,Y_4,T} \cdot \left(\frac{\partial Y_5}{\partial Y_3}\right)_{q,T} \tag{75}$$

$$\left(\frac{\partial f_2}{\partial T}\right)_{q,Y_3} = \left(\frac{\partial f_2}{\partial T}\right)_{q,Y_1,Y_2,Y_3,Y_4,Y_5} + \left(\frac{\partial f_2}{\partial Y_1}\right)_{q,Y_2,Y_3,Y_4,Y_5,T} \cdot \left(\frac{\partial Y_1}{\partial T}\right)_{q,Y_3} + \left(\frac{\partial f_2}{\partial Y_2}\right)_{q,Y_1,Y_3,Y_4,Y_5,T} \cdot \left(\frac{\partial Y_2}{\partial T}\right)_{q,Y_3} + \left(\frac{\partial f_2}{\partial Y_4}\right)_{q,Y_1,Y_2,Y_3,Y_5,T} \cdot \left(\frac{\partial Y_4}{\partial T}\right)_{q,Y_3} + \left(\frac{\partial f_2}{\partial Y_5}\right)_{q,Y_1,Y_2,Y_3,Y_4,T} \cdot \left(\frac{\partial Y_5}{\partial T}\right)_{q,Y_3} \tag{76}$$

Despite their deceptive complexity, these expressions become peculiarly simple, as detailed next.

The jacobian partial derivatives (73)–(76) depend upon the four derivatives

$$\left(\frac{\partial Y_4}{\partial Y_3}\right)_{q,T}, \quad \left(\frac{\partial Y_4}{\partial T}\right)_{q,Y_3}, \quad \left(\frac{\partial Y_5}{\partial Y_3}\right)_{q,T}, \quad \left(\frac{\partial Y_5}{\partial T}\right)_{q,Y_3} \tag{77}$$

which are directly computed by differentiating the mass-action equations (53)–(54) and mass-fraction equations (58)–(59) and then solving for the required derivatives. With such a procedure, these derivatives become

$$\left(\frac{\partial Y_4}{\partial Y_3}\right)_{q,T} = -\frac{2\alpha_{13}Y_4}{Y_1+2Y_4}, \quad \left(\frac{\partial Y_4}{\partial T}\right)_{q,Y_3} = -\frac{Y_1Y_4}{Y_1+2Y_4}\frac{\mathrm{d}G_1}{\mathrm{d}T} \tag{78}$$

and

$$\left(\frac{\partial Y_5}{\partial Y_3}\right)_{q,T} = -\frac{2\alpha_{23}Y_5}{Y_2+2Y_5}, \quad \left(\frac{\partial Y_5}{\partial T}\right)_{q,Y_3} = -\frac{Y_2Y_5}{Y_2+2Y_5}\frac{\mathrm{d}G_2}{\mathrm{d}T} \tag{79}$$

These simple expressions depend upon the mass fractions Y_1, Y_4, Y_2 and Y_5 and never become indeterminate. This is because the denominators constantly remain positive since Y_1 and Y_4 as well as Y_2 and Y_5 never vanish simultaneously.

With these results, the four partial derivatives

$$\left(\frac{\partial Y_1}{\partial Y_3}\right)_{q,T}, \quad \left(\frac{\partial Y_1}{\partial T}\right)_{q,Y_3}, \quad \left(\frac{\partial Y_2}{\partial Y_3}\right)_{q,T}, \quad \left(\frac{\partial Y_2}{\partial T}\right)_{q,Y_3} \tag{80}$$

originate from differentiating (58)–(59) as

$$\left(\frac{\partial Y_1}{\partial Y_3}\right)_{q,T} = \left(\frac{\partial Y_1}{\partial Y_3}\right)_{Y_4} + \left(\frac{\partial Y_1}{\partial Y_4}\right)_{Y_3}\left(\frac{\partial Y_4}{\partial Y_3}\right)_{q,T} = -\frac{\alpha_{13}Y_1}{Y_1+2Y_4} \tag{81}$$

$$\left(\frac{\partial Y_1}{\partial T}\right)_{q,Y_3} = \left(\frac{\partial Y_1}{\partial Y_4}\right)_{Y_3}\left(\frac{\partial Y_4}{\partial T}\right)_{q,Y_3} = \frac{Y_1Y_4}{Y_1+2Y_4}\frac{\mathrm{d}G_1}{\mathrm{d}T} \tag{82}$$

$$\left(\frac{\partial Y_2}{\partial Y_3}\right)_{q,T} = \left(\frac{\partial Y_2}{\partial Y_3}\right)_{Y_5} + \left(\frac{\partial Y_2}{\partial Y_5}\right)_{Y_3}\left(\frac{\partial Y_5}{\partial Y_3}\right)_{q,T} = -\frac{\alpha_{23}Y_2}{Y_2+2Y_5} \tag{83}$$

$$\left(\frac{\partial Y_2}{\partial T}\right)_{q,Y_3} = \left(\frac{\partial Y_2}{\partial Y_5}\right)_{Y_3}\left(\frac{\partial Y_5}{\partial T}\right)_{q,Y_3} = \frac{Y_2Y_5}{Y_2+2Y_5}\frac{\mathrm{d}G_2}{\mathrm{d}T} \tag{84}$$

Consequently, the expressions for the partial derivatives (73)–(76) of f_1 and f_2 with respect to Y_3 and T become

$$\begin{aligned}\left(\frac{\partial f_1}{\partial Y_3}\right)_{q,T} &= 1 - \frac{Y_3-f_1}{2Y_4}\left(-\frac{2\alpha_{13}Y_4}{Y_1+2Y_4}\right) - \frac{Y_3-f_1}{2Y_5}\left(-\frac{2\alpha_{23}Y_5}{Y_2+2Y_5}\right)\\ &= 1 + (Y_3-f_1)\left(\frac{\alpha_{13}}{Y_1+2Y_4} + \frac{\alpha_{23}}{Y_2+2Y_5}\right)\end{aligned} \tag{85}$$

$$\left(\frac{\partial f_1}{\partial T}\right)_{q,Y_3} = -\frac{Y_3 - f_1}{2}\frac{\mathrm{d}G_3}{\mathrm{d}T} - \frac{Y_3 - f_1}{2Y_4}\left(-\frac{Y_1 Y_4}{Y_1 + 2Y_4}\frac{\mathrm{d}G_1}{\mathrm{d}T}\right) - \frac{Y_3 - f_1}{2Y_5}\left(-\frac{Y_2 Y_5}{Y_2 + 2Y_5}\frac{\mathrm{d}G_2}{\mathrm{d}T}\right)$$

$$= \frac{(Y_3 - f_1)}{2}\left(\frac{Y_1}{Y_1 + 2Y_4}\frac{\mathrm{d}G_1}{\mathrm{d}T} + \frac{Y_2}{Y_2 + 2Y_5}\frac{\mathrm{d}G_2}{\mathrm{d}T} - \frac{\mathrm{d}G_3}{\mathrm{d}T}\right) \tag{86}$$

$$\left(\frac{\partial f_2}{\partial Y_3}\right)_{q,T} = -Tc_{v_3} - \frac{\theta_3^v/M_3}{\exp(\theta_3^v/T) - 1} - h_3^0$$

$$+ (Tc_{v_1} + h_1^0)\frac{\alpha_{13} Y_1}{Y_1 + 2Y_4} + (Tc_{v_2} + h_2^0)\frac{\alpha_{23} Y_2}{Y_2 + 2Y_5}$$

$$+ \left(Tc_{v_4} + \frac{\theta_4^v/M_4}{\exp(\theta_4^v/T) - 1}\right)\frac{2\alpha_{13} Y_4}{Y_1 + 2Y_4}$$

$$+ \left(Tc_{v_5} + \frac{\theta_5^v/M_5}{\exp(\theta_5^v/T) - 1}\right)\frac{2\alpha_{23} Y_5}{Y_2 + 2Y_5} \tag{87}$$

$$\left(\frac{\partial f_2}{\partial T}\right)_{q,Y_3} = -\sum_{i=1}^{5} c_{v_i} Y_i - \sum_{i=3}^{5} \frac{Y_i(\theta_i^v/M_i)(\theta_i^v/T^2)\exp(\theta_i^v/T)}{(\exp(\theta_i^v/T) - 1)^2}$$

$$- (Tc_{v_1} + h_1^0)\frac{Y_1 Y_4}{Y_1 + 2Y_4}\frac{\mathrm{d}G_1}{\mathrm{d}T} - (Tc_{v_2} + h_2^0)\frac{Y_2 Y_5}{Y_2 + 2Y_5}\frac{\mathrm{d}G_2}{\mathrm{d}T}$$

$$+ \left(Tc_{v_4} + \frac{\theta_4^v/M_4}{\exp(\theta_4^v/T) - 1}\right)\frac{Y_1 Y_4}{Y_1 + 2Y_4}\frac{\mathrm{d}G_1}{\mathrm{d}T}$$

$$+ \left(Tc_{v_5} + \frac{\theta_5^v/M_5}{\exp(\theta_5^v/T) - 1}\right)\frac{Y_2 Y_5}{Y_2 + 2Y_5}\frac{\mathrm{d}G_2}{\mathrm{d}T} \tag{88}$$

With these analytical partial derivatives, the procedure for determining temperature, and the five mass fractions is theoretically complete. Therefore, a practical implementation utilizes expressions (62)–(63) and (58)–(59) to compute Y_i, $i \neq 3$, for a given state (ρ, ε) at each grid point and associated (Y_3, T). All of these variables are then employed to evaluate functions (66)–(67) and all the corresponding partial derivatives for the Netwton's-algorithm determination of Y_3 and T. The computational results discussed in Section 12 indicate that this procedure quadratically converges, in two or three iterations, and directly yields temperature and the five mass fractions. Pressure is then explicitly computed using (49).

6. PARTIAL DERIVATIVES OF T, Y_1, Y_2, Y_3, Y_4, Y_5 WITH RESPECT TO ρ AND ε

From the EOS (49), the thermodynamic and jacobian partial derivatives of pressure depend on the partial derivatives of temperature T and mass fractions Y_i, $1 \leqslant i \leqslant 5$ with respect

to ρ and ε. This section presents these derivatives. The derivatives of Y_3 and T are exactly determined from differentiating system (68). The derivatives of Y_1, Y_2, Y_4, Y_5 then follow from differentiating their defining expressions.

6.1. Derivatives of T and Y_3

Considering that $Q = Q(\rho, \varepsilon)$, the differential of both sides of expression (68) yields

$$\left(\left[\left(\frac{\partial F}{\partial Q} \right)_{\rho,\varepsilon} \right] \left(\frac{\partial Q}{\partial \rho} \right)_{\varepsilon} + \left(\frac{\partial F}{\partial \rho} \right)_{Q,\varepsilon} \right) \mathrm{d}\rho + \left(\left[\left(\frac{\partial F}{\partial Q} \right)_{\rho,\varepsilon} \right] \left(\frac{\partial Q}{\partial \varepsilon} \right)_{\rho} + \left(\frac{\partial F}{\partial \varepsilon} \right)_{Q,\rho} \right) \mathrm{d}\varepsilon = 0 \tag{89}$$

This constitutes a linear combination of the linearly independent differentials $\mathrm{d}\rho$ and $\mathrm{d}\varepsilon$, which holds true if and only if their coefficients independently vanish, which defines the two linear systems

$$\left(\frac{\partial Q}{\partial \rho} \right)_{\varepsilon} = - \left[\left(\frac{\partial F}{\partial Q} \right)_{\rho,\varepsilon} \right]^{-1} \left(\frac{\partial F}{\partial \rho} \right)_{Q,\varepsilon}, \quad \left(\frac{\partial Q}{\partial \varepsilon} \right)_{\rho} = - \left[\left(\frac{\partial F}{\partial Q} \right)_{\rho,\varepsilon} \right]^{-1} \left(\frac{\partial F}{\partial \varepsilon} \right)_{Q,\rho} \tag{90}$$

The jacobian in both of these expressions is invariant and coincides with that in (69) at convergence, Systems (90) thus directly supply the partial derivatives

$$\left(\frac{\partial Y_3}{\partial \rho} \right)_{\varepsilon}, \quad \left(\frac{\partial Y_3}{\partial \varepsilon} \right)_{\rho}, \quad \left(\frac{\partial T}{\partial \rho} \right)_{\varepsilon}, \quad \left(\frac{\partial T}{\partial \varepsilon} \right)_{\rho} \tag{91}$$

Systems (90) depend on the partial derivatives

$$\left(\frac{\partial F}{\partial \rho} \right)_{Q,\varepsilon}, \quad \left(\frac{\partial F}{\partial \varepsilon} \right)_{Q,\rho} \tag{92}$$

which are expressed as

$$\left(\frac{\partial f_1}{\partial \rho} \right)_{Y_3,T,\varepsilon} = \left(\frac{\partial f_1}{\partial Y_4} \right)_{q,Y_3,Y_5,T} \left(\frac{\partial Y_4}{\partial \rho} \right)_{Y_3,T} + \left(\frac{\partial f_1}{\partial Y_5} \right)_{q,Y_3,Y_4,T} \left(\frac{\partial Y_5}{\partial \rho} \right)_{Y_3,T} \tag{93}$$

$$\left(\frac{\partial f_1}{\partial \varepsilon} \right)_{Y_3,T,\rho} = 0.0 \tag{94}$$

$$\begin{aligned} \left(\frac{\partial f_2}{\partial \rho} \right)_{Y_3,T,\varepsilon} = {} & \left(\frac{\partial f_2}{\partial Y_1} \right)_{q,Y_2,Y_3,Y_4,Y_5,T} \left(\frac{\partial Y_1}{\partial \rho} \right)_{Y_3,T} + \left(\frac{\partial f_2}{\partial Y_2} \right)_{q,Y_1,Y_3,Y_4,Y_5,T} \left(\frac{\partial Y_2}{\partial \rho} \right)_{Y_3,T} \\ & + \left(\frac{\partial f_2}{\partial Y_4} \right)_{q,Y_1,Y_2,Y_3,Y_5,T} \left(\frac{\partial Y_4}{\partial \rho} \right)_{Y_3,T} + \left(\frac{\partial f_2}{\partial Y_5} \right)_{q,Y_1,Y_2,Y_3,Y_4,T} \left(\frac{\partial Y_5}{\partial \rho} \right)_{Y_3,T} \end{aligned} \tag{95}$$

$$\left(\frac{\partial f_2}{\partial \varepsilon} \right)_{Y_3,T,\rho} = \left(\frac{\partial f_2}{\partial \varepsilon} \right)_{Y_1,Y_2,Y_3,Y_4,Y_5,T,\rho} = 1.0 \tag{96}$$

These relationships depend on the partial derivatives

$$\left(\frac{\partial f_1}{\partial Y_i}\right)_{q,Y_j,T}, \quad \left(\frac{\partial f_2}{\partial Y_i}\right)_{q,Y_j,T}, \ i \neq j \tag{97}$$

and

$$\left(\frac{\partial Y_4}{\partial \rho}\right)_{Y_3,T}, \quad \left(\frac{\partial Y_5}{\partial \rho}\right)_{Y_3,T}, \quad \left(\frac{\partial Y_1}{\partial \rho}\right)_{Y_3,T}, \quad \left(\frac{\partial Y_2}{\partial \rho}\right)_{Y_3,T} \tag{98}$$

At convergence of (69), the derivatives of f_1 and f_2 in (97) directly follow from the corresponding ones within (85)–(86), after setting $f_1 = 0$ and $f_2 = 0$. The derivatives of Y_4 and Y_5 in (98) are obtained from directly differentiating the mass-action equations (53)–(54). With this procedure, the mass-fraction derivatives (98) become

$$\left(\frac{\partial Y_4}{\partial \rho}\right)_{Y_3,T} = \frac{1}{\rho}\frac{Y_1 Y_4}{Y_1 + 2Y_4}, \quad \left(\frac{\partial Y_5}{\partial \rho}\right)_{Y_3,T} = \frac{1}{\rho}\frac{Y_2 Y_5}{Y_2 + 2Y_5} \tag{99}$$

The partial derivatives of Y_1 and Y_2 then directly follow from differentiating the mass-fraction equations (58)–(59) as

$$\left(\frac{\partial Y_1}{\partial \rho}\right)_{Y_3,T} = -\frac{1}{\rho}\frac{Y_1 Y_4}{Y_1 + 2Y_4}, \quad \left(\frac{\partial Y_2}{\partial \rho}\right)_{Y_3,T} = -\frac{1}{\rho}\frac{Y_2 Y_5}{Y_2 + 2Y_5} \tag{100}$$

With expressions (99)–(100), the partial derivatives of f_1 and f_2 become

$$\left(\frac{\partial f_1}{\partial \rho}\right)_{Y_3,T,\varepsilon} = -\frac{1}{2\rho}\frac{Y_1 Y_3}{Y_1 + 2Y_4} - \frac{1}{2\rho}\frac{Y_2 Y_3}{Y_2 + 2Y_5} \tag{101}$$

$$\left(\frac{\partial f_1}{\partial \varepsilon}\right)_{Y_3,T,\rho} = 0.0 \tag{102}$$

$$\begin{aligned}\left(\frac{\partial f_2}{\partial \rho}\right)_{Y_3,T,\varepsilon} &= \left(Tc_{v_1} + h_1^0\right)\frac{1}{\rho}\frac{Y_1 Y_4}{Y_1 + 2Y_4} + \left(Tc_{v_2} + h_2^0\right)\frac{1}{\rho}\frac{Y_2 Y_5}{Y_2 + 2Y_5} \\ &\quad - \left(Tc_{v_4} + \frac{\theta_4^v/M_4}{\exp(\theta_4^v/T) - 1}\right)\frac{1}{\rho}\frac{Y_1 Y_4}{Y_1 + 2Y_4} \\ &\quad - \left(Tc_{v_5} + \frac{\theta_5^v/M_5}{\exp(\theta_5^v/T) - 1}\right)\frac{1}{\rho}\frac{Y_2 Y_5}{Y_2 + 2Y_5}\end{aligned} \tag{103}$$

$$\left(\frac{\partial f_2}{\partial \varepsilon}\right)_{Y_3,T,\rho} = 1.0 \tag{104}$$

6.2. Derivatives of Y_1, Y_2, Y_4, Y_5

Once the derivatives of T and Y_3 with respect to ρ and ε have been calculated, the partial derivatives

$$\left(\frac{\partial Y_4}{\partial \rho}\right)_\varepsilon, \quad \left(\frac{\partial Y_4}{\partial \varepsilon}\right)_\rho, \quad \left(\frac{\partial Y_5}{\partial \rho}\right)_\varepsilon, \quad \left(\frac{\partial Y_5}{\partial \varepsilon}\right)_\rho \tag{105}$$

can then be exactly determined. Given the functional relations (64)–(65) for Y_i, $i \neq 3$, these derivatives are expressed as

$$\left(\frac{\partial Y_4}{\partial \rho}\right)_\varepsilon = \left(\frac{\partial Y_4}{\partial Y_3}\right)_{\rho,T} \left(\frac{\partial Y_3}{\partial \rho}\right)_\varepsilon + \left(\frac{\partial Y_4}{\partial T}\right)_{\rho,Y_3} \left(\frac{\partial T}{\partial \rho}\right)_\varepsilon + \left(\frac{\partial Y_4}{\partial \rho}\right)_{Y_3,T} \tag{106}$$

$$\left(\frac{\partial Y_4}{\partial \varepsilon}\right)_\rho = \left(\frac{\partial Y_4}{\partial Y_3}\right)_{\rho,T} \left(\frac{\partial Y_3}{\partial \varepsilon}\right)_\rho + \left(\frac{\partial Y_4}{\partial T}\right)_{\rho,Y_3} \left(\frac{\partial T}{\partial \varepsilon}\right)_\rho \tag{107}$$

$$\left(\frac{\partial Y_5}{\partial \rho}\right)_\varepsilon = \left(\frac{\partial Y_5}{\partial Y_3}\right)_{\rho,T} \left(\frac{\partial Y_3}{\partial \rho}\right)_\varepsilon + \left(\frac{\partial Y_5}{\partial T}\right)_{\rho,Y_3} \left(\frac{\partial T}{\partial \rho}\right)_\varepsilon + \left(\frac{\partial Y_5}{\partial \rho}\right)_{Y_3,T} \tag{108}$$

$$\left(\frac{\partial Y_5}{\partial \varepsilon}\right)_\rho = \left(\frac{\partial Y_5}{\partial Y_3}\right)_{\rho,T} \left(\frac{\partial Y_3}{\partial \varepsilon}\right)_\rho + \left(\frac{\partial Y_5}{\partial T}\right)_{\rho,Y_3} \left(\frac{\partial T}{\partial \varepsilon}\right)_\rho \tag{109}$$

where the partial derivatives of Y_4 and Y_5 with respect to Y_3 and T are detailed in Section 6.1. Hence, expressions (105) become

$$\left(\frac{\partial Y_4}{\partial \rho}\right)_\varepsilon = -\frac{2\alpha_{13} Y_4}{Y_1 + 2Y_4} \left(\frac{\partial Y_3}{\partial \rho}\right)_\varepsilon - \frac{Y_1 Y_4}{Y_1 + 2Y_4} \frac{\mathrm{d}G_1}{\mathrm{d}T} \left(\frac{\partial T}{\partial \rho}\right)_\varepsilon + \frac{1}{\rho} \frac{Y_1 Y_4}{Y_1 + 2Y_4} \tag{110}$$

$$\left(\frac{\partial Y_4}{\partial \varepsilon}\right)_\rho = -\frac{2\alpha_{13} Y_4}{Y_1 + 2Y_4} \left(\frac{\partial Y_3}{\partial \varepsilon}\right)_\rho - \frac{Y_1 Y_4}{Y_1 + 2Y_4} \frac{\mathrm{d}G_1}{\mathrm{d}T} \left(\frac{\partial T}{\partial \varepsilon}\right)_\rho \tag{111}$$

$$\left(\frac{\partial Y_5}{\partial \rho}\right)_\varepsilon = -\frac{2\alpha_{23} Y_5}{Y_2 + 2Y_5} \left(\frac{\partial Y_3}{\partial \rho}\right)_\varepsilon - \frac{Y_2 Y_5}{Y_2 + 2Y_5} \frac{\mathrm{d}G_2}{\mathrm{d}T} \left(\frac{\partial T}{\partial \rho}\right)_\varepsilon + \frac{1}{\rho} \frac{Y_2 Y_5}{Y_2 + 2Y_5} \tag{112}$$

$$\left(\frac{\partial Y_5}{\partial \varepsilon}\right)_\rho = -\frac{2\alpha_{23} Y_5}{Y_2 + 2Y_5} \left(\frac{\partial Y_3}{\partial \varepsilon}\right)_\rho - \frac{Y_2 Y_5}{Y_2 + 2Y_5} \frac{\mathrm{d}G_2}{\mathrm{d}T} \left(\frac{\partial T}{\partial \varepsilon}\right)_\rho \tag{113}$$

With these expressions, along with (58)–(59) the partial derivatives

$$\left(\frac{\partial Y_1}{\partial \rho}\right)_\varepsilon, \quad \left(\frac{\partial Y_1}{\partial \varepsilon}\right)_\rho, \quad \left(\frac{\partial Y_2}{\partial \rho}\right)_\varepsilon, \quad \left(\frac{\partial Y_2}{\partial \varepsilon}\right)_\rho \tag{114}$$

are developed as

$$\left(\frac{\partial Y_1}{\partial \rho}\right)_\varepsilon = -\left(\frac{\partial Y_4}{\partial \rho}\right)_\varepsilon - \alpha_{13}\left(\frac{\partial Y_3}{\partial \rho}\right)_\varepsilon$$

$$= \frac{-\alpha_{13} Y_1}{Y_1 + 2Y_4}\left(\frac{\partial Y_3}{\partial \rho}\right)_\varepsilon + \frac{Y_1 Y_4}{Y_1 + 2Y_4}\frac{\mathrm{d}G_1}{\mathrm{d}T}\left(\frac{\partial T}{\partial \rho}\right)_\varepsilon - \frac{1}{\rho}\frac{Y_1 Y_4}{Y_1 + 2Y_4} \tag{115}$$

$$\left(\frac{\partial Y_1}{\partial \varepsilon}\right)_\rho = -\left(\frac{\partial Y_4}{\partial \varepsilon}\right)_\rho - \alpha_{13}\left(\frac{\partial Y_3}{\partial \varepsilon}\right)_\rho$$

$$= \frac{-\alpha_{13} Y_1}{Y_1 + 2Y_4}\left(\frac{\partial Y_3}{\partial \varepsilon}\right)_\rho + \frac{Y_1 Y_4}{Y_1 + 2Y_4}\frac{\mathrm{d}G_1}{\mathrm{d}T}\left(\frac{\partial T}{\partial \varepsilon}\right)_\rho \tag{116}$$

$$\left(\frac{\partial Y_2}{\partial \rho}\right)_\varepsilon = -\left(\frac{\partial Y_5}{\partial \rho}\right)_\varepsilon - \alpha_{23}\left(\frac{\partial Y_3}{\partial \rho}\right)_\varepsilon$$

$$= \frac{-\alpha_{23} Y_2}{Y_2 + 2Y_5}\left(\frac{\partial Y_3}{\partial \rho}\right)_\varepsilon + \frac{Y_2 Y_5}{Y_2 + 2Y_5}\frac{\mathrm{d}G_2}{\mathrm{d}T}\left(\frac{\partial T}{\partial \rho}\right)_\varepsilon - \frac{1}{\rho}\frac{Y_2 Y_5}{Y_2 + 2Y_5} \tag{117}$$

$$\left(\frac{\partial Y_2}{\partial \varepsilon}\right)_\rho = -\left(\frac{\partial Y_5}{\partial \varepsilon}\right)_\rho - \alpha_{23}\left(\frac{\partial Y_3}{\partial \varepsilon}\right)_\rho$$

$$= \frac{-\alpha_{23} Y_2}{Y_2 + 2Y_5}\left(\frac{\partial Y_3}{\partial \varepsilon}\right)_\rho + \frac{Y_2 Y_5}{Y_2 + 2Y_5}\frac{\mathrm{d}G_2}{\mathrm{d}T}\left(\frac{\partial T}{\partial \varepsilon}\right)_\rho \tag{118}$$

7. PRESSURE AND ITS THERMODYNAMIC DERIVATIVES

With the calculated temperature and mass fractions, pressure is readily calculated via the EOS

$$p = \rho T \sum_{i=1}^{5} \frac{Y_i}{M_i} \tag{119}$$

The thermodynamic derivatives of pressure are then exactly determined by differentiating this EOS in the form

$$\left(\frac{\partial p}{\partial \rho}\right)_\varepsilon = T\sum_{i=1}^{5}\frac{Y_i}{M_i} + \rho\left(\frac{\partial T}{\partial \rho}\right)_\varepsilon \sum_{i=1}^{5}\frac{Y_i}{M_i} + \rho T\sum_{i=1}^{5}\frac{1}{M_i}\left(\frac{\partial Y_i}{\partial \rho}\right)_\varepsilon \tag{120}$$

$$\left(\frac{\partial p}{\partial \varepsilon}\right)_\rho = \rho\left(\frac{\partial T}{\partial \varepsilon}\right)_\rho \sum_{i=1}^{5}\frac{Y_i}{M_i} + \rho T\sum_{i=1}^{5}\frac{1}{M_i}\left(\frac{\partial Y_i}{\partial \varepsilon}\right)_\rho \tag{121}$$

which shows dependence on the thermodynamic derivatives of both T and mass fractions Y_i, $1 \leqslant i \leqslant 5$, with respect to ρ and ε.

8. JACOBIAN PARTIAL DERIVATIVES OF PRESSURE AND TEMPERATURE

The convergence of implicit Euler and Navier–Stokes CFD algorithms also depends upon accurate and continuous jacobians of pressure with respect to the state variable q, Reference [5]. Implicit Navier–Stokes CFD algorithms also require accurate and continuous jacobians of temperature with respect to q. This section exactly determines these derivatives.

An application of the chain rule to the EOS in (7), $p = p(\rho, \varepsilon(q))$, leads to the partial derivatives of pressure with respect to the flow variable $q \equiv \{\rho, \boldsymbol{m}, E\}^{\mathrm{T}}$ as

$$\left(\frac{\partial p}{\partial \rho}\right)_{\boldsymbol{m},E} = \left(\frac{\partial p}{\partial \rho}\right)_{\varepsilon} + \left(\frac{\partial p}{\partial \varepsilon}\right)_{\rho} \left(\frac{\partial \varepsilon}{\partial \rho}\right)_{\boldsymbol{m},E}$$

$$= \left(\frac{\partial p}{\partial \rho}\right)_{\varepsilon} + \left(\frac{\partial p}{\partial \varepsilon}\right)_{\rho} \frac{1}{\rho^2} \left(\frac{1}{\rho} \sum_{i=1}^{n} m_i m_i - E\right) \tag{122}$$

$$\left(\frac{\partial p}{\partial m_i}\right)_{\rho,m_j,E,i\neq j} = \left(\frac{\partial p}{\partial \varepsilon}\right)_{\rho} \left(\frac{\partial \varepsilon}{\partial m_i}\right)_{\rho,m_j,E,i\neq j} = \left(\frac{\partial p}{\partial \varepsilon}\right)_{\rho} \left(-\frac{m_i}{\rho^2}\right) \tag{123}$$

$$\left(\frac{\partial p}{\partial E}\right)_{\rho,\boldsymbol{m}} = \left(\frac{\partial p}{\partial \varepsilon}\right)_{\rho} \left(\frac{\partial \varepsilon}{\partial E}\right)_{\rho,\boldsymbol{m}} = \left(\frac{\partial p}{\partial \varepsilon}\right)_{\rho} \left(\frac{1}{\rho}\right) \tag{124}$$

These results also show that the derivatives of pressure with respect to m_i, $1 \leqslant i \leqslant 3$, and E linearly depend upon one another as

$$\left(\frac{\partial p}{\partial m_i}\right)_{\rho,m_j,E,i\neq j} + \frac{m_i}{\rho} \left(\frac{\partial p}{\partial E}\right)_{\rho,\boldsymbol{m}} = 0 \tag{125}$$

The corresponding Jacobian partial derivatives of T are directly obtained by replacing p with T in (122)–(124). As noted in Section 4, Equations (58)–(59), (62)–(63), and (66)–(67) asymptotically approach perfect-gas expressions. Therefore (122)–(124) will converge for low temperatures to perfect-gas partial derivatives. In any case, these jacobian derivatives depend on the thermodynamic derivatives $(\partial p/\partial \rho)_{\varepsilon}$ and $(\partial p/\partial \varepsilon)_{\rho}$. Similarly, the jacobian partial derivatives of T depend on the thermodynamic derivatives $(\partial T/\partial \rho)_{\varepsilon}$ and $(\partial T/\partial \varepsilon)_{\rho}$.

9. THERMODYNAMIC PROPERTIES WITH P AND T AS INDEPENDENT VARIABLES

The procedure described in Sections 4–6 generates the thermodynamic properties of air with density and internal energy as independent variables. This set of independent variables is eminently suited for CFD applications, for, as indicated in Section 2, these variables are readily available from the dependent state variable q in the Euler and Navier–Stokes conservation law systems. The same procedure, however, can also deliver thermodynamic properties for any

other set of independent variables because the procedure also delivers partial derivatives. This section presents a rapidly converging Newton's method to use the procedure in Sections 4–6 to generate thermodynamic properties with p and T as independent variables. The method can also be swiftly modified to generate thermodynamic properties for any other set of independent thermodynamic variables.

The procedure in Sections 4–6 delivers the functions $p = p(\rho, \varepsilon)$, $T = T(\rho, \varepsilon)$ and their partial derivatives with respect to ρ and ε. The expressions for the differentials of $p = p(\rho, \varepsilon)$ and $T = T(\rho, \varepsilon)$ are

$$\mathrm{d}p = \left(\frac{\partial p}{\partial \rho}\right)_{\varepsilon} \mathrm{d}\rho + \left(\frac{\partial p}{\partial \varepsilon}\right)_{\rho} \mathrm{d}\varepsilon, \quad \mathrm{d}T = \left(\frac{\partial T}{\partial \rho}\right)_{\varepsilon} \mathrm{d}\rho + \left(\frac{\partial T}{\partial \varepsilon}\right)_{\rho} \mathrm{d}\varepsilon \tag{126}$$

Upon setting the differentials in these expressions equal to first-order variations and solving for the variations $\Delta\rho$ and $\Delta\varepsilon$, the following expressions emerge

$$\Delta\rho = \frac{\left(\dfrac{\partial T}{\partial \varepsilon}\right)_{\rho} \Delta p - \left(\dfrac{\partial p}{\partial \varepsilon}\right)_{\rho} \Delta T}{\left(\dfrac{\partial p}{\partial \rho}\right)_{\varepsilon}\left(\dfrac{\partial T}{\partial \varepsilon}\right)_{\rho} - \left(\dfrac{\partial T}{\partial \rho}\right)_{\varepsilon}\left(\dfrac{\partial p}{\partial \varepsilon}\right)_{\rho}}, \quad \Delta\varepsilon = \frac{-\left(\dfrac{\partial T}{\partial \rho}\right)_{\varepsilon} \Delta p + \left(\dfrac{\partial p}{\partial \rho}\right)_{\varepsilon} \Delta T}{\left(\dfrac{\partial p}{\partial \rho}\right)_{\varepsilon}\left(\dfrac{\partial T}{\partial \varepsilon}\right)_{\rho} - \left(\dfrac{\partial T}{\partial \rho}\right)_{\varepsilon}\left(\dfrac{\partial p}{\partial \varepsilon}\right)_{\rho}} \tag{127}$$

The variations $\Delta\rho$ and $\Delta\varepsilon$ remain well defined since the denominator in these results never vanishes. Set all the variations in these results equal to the expressions

$$\Delta p = p_0 - p^i, \quad \Delta T = T_0 - T^i, \quad \Delta\rho = \rho^{i+1} - \rho^i, \quad \Delta\varepsilon = \varepsilon^{i+1} - \varepsilon^i \tag{128}$$

In these expressions, p_0 and T_0 denote prescribed pressure and temperature; p^i and T^i correspond to the pressure and temperature the procedure delivers in relation to ρ^i and ε^i. Hence ρ^{i+1} and ε^{i+1} calculated through (127) represent the refinements on ρ and ε as p^i and T^i respectively converge toward p_0 and T_0. Since the expressions in (127) correspond to Newton's method on the system of functions $p(\rho, \varepsilon) - p_0 = 0$ and $T(\rho, \varepsilon) - T_0 = 0$ the method has been found to converge quadratically in two or three iterations, provided that the initial estimate for ρ and ε lie within the range of convergence and the absolute value of ρ^{i+1} and ε^{i+1} are used in each cycle, following the indications in Section 5. With the procedure described in Sections 4–6 encapsulated in a subroutine, the iteration corresponding to Equations (127) finds its realization with two or three calls to such a subroutine. At convergence, $\Delta\rho \to 0$, $\Delta\varepsilon \to 0$, and $p^i \to p_0$, $T^i \to T_0$, hence the procedure effectively provides thermodynamic properties for prescribed p and T.

10. SPECIFIC HEATS c_v AND c_p

The mixture specific heat at constant volume c_v evolves from the derivative of the internal energy ε with respect to temperature. The specific heat at constant pressure c_p follows in terms of c_v. By definition, the expressions for c_v and c_p are

$$c_v = \left(\frac{\partial \varepsilon}{\partial T}\right)_{\rho}, \quad c_p = \left(\frac{\partial h}{\partial T}\right)_{p} \tag{129}$$

From the developments in Reference [14], these two derivatives can then be expressed in terms of the derivatives of only one thermodynamic variable as

$$c_v = \left(\frac{\partial T}{\partial \varepsilon}\right)_\rho^{-1}, \quad c_p = c_v - \frac{T}{\rho^2 \left(\frac{\partial T}{\partial p}\right)_\rho \left(\frac{\partial T}{\partial \rho}\right)_p}, \quad c_p = c_v + \frac{T\left(\frac{\partial p}{\partial T}\right)_\rho^2}{\rho^2 \left(\frac{\partial p}{\partial \rho}\right)_T} \tag{130}$$

where the derivatives in these expressions are calculated following the methods in Section 5.

The ratio of specific heats then follows as

$$\gamma = \frac{c_p}{c_v} = \left(\frac{\partial h}{\partial T}\right)_p \left(\frac{\partial T}{\partial \varepsilon}\right)_\rho = 1 - \frac{T\left(\frac{\partial T}{\partial \varepsilon}\right)_\rho}{\rho^2 \left(\frac{\partial T}{\partial p}\right)_\rho \left(\frac{\partial T}{\partial \rho}\right)_p} \tag{131}$$

In the absence of chemical reactions, $M = \text{constant}$ and the derivatives of pressure from (10) reduce (130) to the well known result

$$c_p = c_v + \frac{\mathscr{R}}{M} \tag{132}$$

11. SPEED OF SOUND

A new and convenient expression for the square of the speed of sound evolves as follows. The square of the isotropic component of all the eigenvalues of the inviscid flux vector in (2) has been determined as [19]

$$c^2 = \left(\frac{\partial p}{\partial \rho}\right)_{\boldsymbol{m},E} + \left(\frac{\partial p}{\partial E}\right)_{\rho,\boldsymbol{m}} \left(\frac{E+p}{\rho} - \frac{1}{\rho^2}\sum_{i=1}^{n} m_i m_i\right) \tag{133}$$

By virtue of the jacobian derivatives of pressure (122)–(124), this expression reduces to

$$c^2 = \left(\frac{\partial p}{\partial \rho}\right)_\varepsilon + \frac{p}{\rho^2}\left(\frac{\partial p}{\partial \varepsilon}\right)_\rho \tag{134}$$

This result coincides with the speed of sound calculated from $p = p(\rho, \varepsilon(\rho, s))$ as

$$c^2 = \left(\frac{\partial p}{\partial \rho}\right)_s = \left(\frac{\partial p}{\partial \rho}\right)_\varepsilon + \left(\frac{\partial p}{\partial \varepsilon}\right)_\rho \left(\frac{\partial \varepsilon}{\partial \rho}\right)_s = \left(\frac{\partial p}{\partial \rho}\right)_\varepsilon + \frac{p}{\rho^2}\left(\frac{\partial p}{\partial \varepsilon}\right)_\rho \tag{135}$$

where the final step derives from the first principle of thermodynamics [14]. The speed of sound, therefore, is calculated with this expression, for the thermodynamic derivatives of pressure are determined as shown in Section 7.

This expression for the square of speed of sound can also be expressed in terms of the specific heat ratio γ using the thermodynamic pressure derivatives and the following equality

from the third expression in (130)

$$\left(\frac{\partial p}{\partial \rho}\right)_T = \gamma \left(\frac{\partial p}{\partial \rho}\right)_T - \frac{T}{c_v \rho^2}\left(\frac{\partial p}{\partial T}\right)_\rho^2 \tag{136}$$

The expression for the square of the speed of sound thus becomes

$$\begin{aligned} c^2 &= \left(\frac{\partial p}{\partial \rho}\right)_T + \left(\frac{\partial p}{\partial T}\right)_\rho \left(\frac{\partial T}{\partial \rho}\right)_\varepsilon + \frac{p}{\rho^2}\left(\frac{\partial p}{\partial T}\right)_\rho \left(\frac{\partial T}{\partial \varepsilon}\right)_\rho \\ &= \gamma \left(\frac{\partial p}{\partial \rho}\right)_T + \left(\frac{\partial p}{\partial T}\right)_\rho \left(\left(\frac{\partial T}{\partial \rho}\right)_\varepsilon + \frac{p}{\rho^2}\left(\frac{\partial T}{\partial \varepsilon}\right)_\rho - \frac{T}{c_v \rho^2}\left(\frac{\partial p}{\partial T}\right)_\rho\right) \\ &= \gamma RT + \gamma \rho T \left(\frac{\partial R}{\partial \rho}\right)_T + \left(\frac{\partial p}{\partial T}\right)_\rho \left(\left(\frac{\partial T}{\partial \rho}\right)_\varepsilon + \frac{p}{c_v \rho^2} - \frac{T}{c_v \rho^2}\left(\frac{\partial p}{\partial T}\right)_\rho\right) \end{aligned} \tag{137}$$

where the EOS (10), with $R \equiv \mathscr{R}/M$, contributed the expression for the derivative of pressure with respect to ρ. In the presence of chemical reactions, therefore, the speed of sound differs from the 'frozen' speed of sound $\sqrt{\gamma RT}$. In the absence of chemical reactions $R =$ constant and with $T = T(\varepsilon)$ and (10) for EOS, the additional terms beyond γRT in (137) vanish and the speed of sound then coincides with $\sqrt{\gamma RT}$.

12. COMPUTATIONAL RESULTS

The procedure detailed in this paper has generated the thermodynamic properties of equilibrium air using as independent thermodynamic variables both density and internal energy, suitable for CFD applications, and pressure and temperature, following the developments in Section 9. The results are generated for the pressure and density ranges that correspond to an increase of altitude in standard atmosphere of 30 000 m, slightly over 98 000 ft, above sea level. Table IV summarizes the reference pressure and density

The symbols ρ_∞ and p_∞ in the following discussion denote sea-level density and pressure.

An electrically neutral five-species model for air remains accurate for temperatures up to about 9000 K [12]. The temperature range used for the results in this section, however, reaches over 10 000 K, in order to verify that at high temperatures the procedure yields results

Table IV. Reference density and pressure.

Altitude (km)	Density (kg m^{-3})	Pressure (Pa)
30	0.0184	1196.968507
24	0.0469	2971.756296
18	0.1216	7565.246266
12	0.3119	19399.475779
6	0.6601	47217.594506
0	1.2250	101325.024000

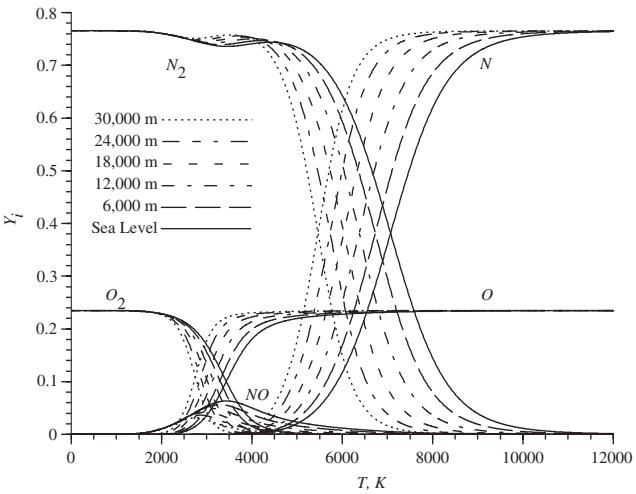

Figure 1. Mass Fractions Y_i versus temperature.

that correspond to a perfect gas of fully dissociated, hence atomic, species. The procedure efficiently generates results that agree with published results. This is seen through the distributions of mole fractions, constant-volume specific heat, and speed of sound respectively in Figures 2, 9 and 12, which virtually coincide with the corresponding curves in References [12, 14].

All variables in this section remain dimensional and are arranged in non-dimensional groupings. The results are presented in sets of isochors for pressure and sets of isobars for mass and mole fractions, mixture molecular mass, temperature, thermodynamic derivatives of pressure and temperature, constant-volume and constant-pressure specific heats, specific heat ratio, and sound speed squared.

Figures 1 and 2 present the distributions versus temperature of species mass and mole fractions. At $p = 1$ atm, the dissociation of molecular oxygen begins above 2000 K and is virtually complete above 4000 K; the dissociation of molecular nitrogen begins above 4000 K, when that of oxygen completes, and is virtually complete over 9000 K; nitric oxide begins to form at about 2000 K; its mole fraction increases, reaches a peak at about 3500 K and then decreases. These features and all the $p = 1$ atm curves virtually coincide with the results reported in Reference [14]. This reference, also confirms the correctness of the shift of the mole fraction curves observed in the figure. A decrease in pressure favours dissociations; they can thus initiate at comparatively lower temperatures, which explains the shift to the left of the mass and mole fraction curves.

These curves show a rapid decrease of N_2. This effect is due to the formation of NO, which requires nitrogen atoms. As dictated by conservation of mass, a relative minimum in N_2 mass fraction, for $T < 4000$ K, corresponds to a maximum in NO mass fraction. The mass fraction of O increases monotonically, whereas the mole fraction decreases from a relative maximum for $T < 5000$ K. Since a mole fraction is the ratio of species moles and mixture moles, this decrease of O mole fraction is not so much due to a decrease in the number of atoms and molecules of oxygen, but rather to a drastic increase of the total number of mixture moles due

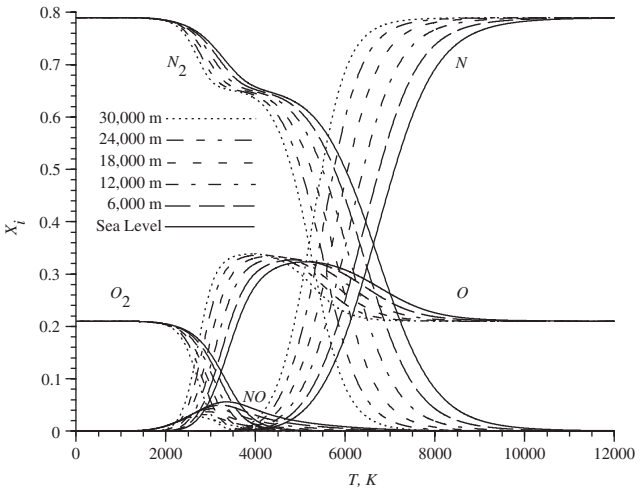

Figure 2. Mole Fractions X_i versus temperature.

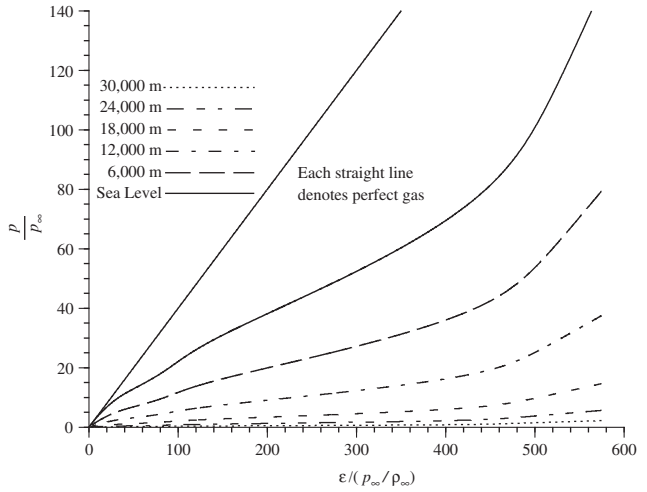

Figure 3. Pressure versus internal energy.

to the rapid dissociation of molecular nitrogen. The results reported in Reference [12] then indicate that electrons and ionic species are virtually absent, for their mole fractions are less than 0.008, for $T < 9000$ K, and $p = 0.01$ atm; even smaller mole fractions of these charged species are present at higher pressure. This observation justifies the selection of an electrically neutral reacting-air model for this temperature range.

For the various density levels in Table IV, Figure 3 shows the variation of pressure versus internal energy, and Figures 4 and 5 present the variations of the thermodynamic partial derivatives of pressure versus temperature.

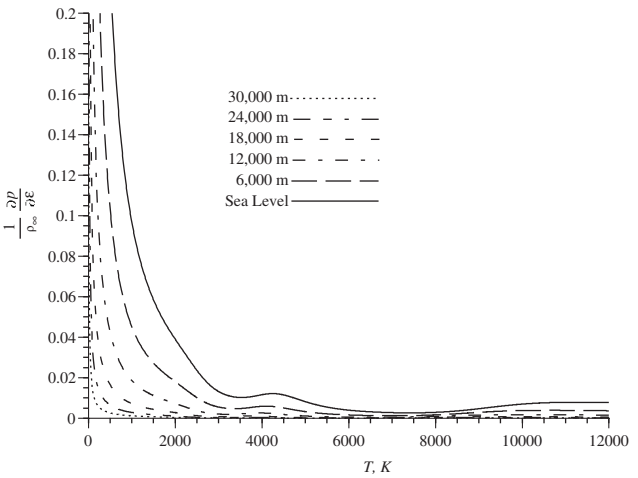

Figure 4. $1/\rho_\infty(\partial p/\partial \varepsilon)_\rho$ versus temperature.

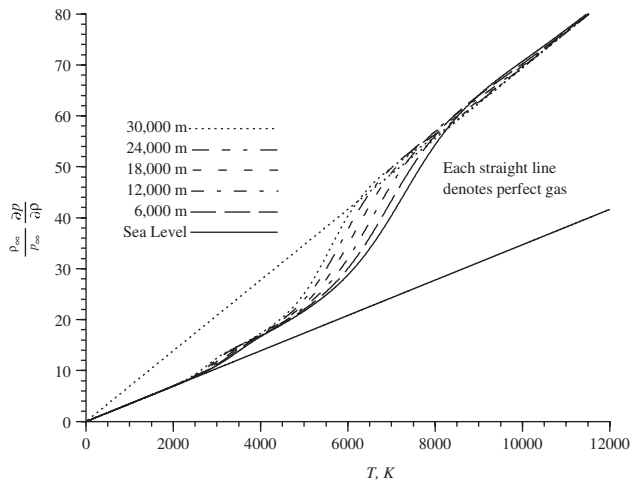

Figure 5. $\rho_\infty/p_\infty(\partial p/\partial \rho)_\varepsilon$ versus temperature.

Pressure is charted versus ε because from the first EOS in (6), pressure linearly increases with ε. This representation clearly shows the difference between perfect- and reacting-air predictions. For a given density, the chart illustrates the incorrect high pressure predictions of the perfect-gas model, which become wholly unrealistic as ε increases. This noticeable discrepancy between perfect- and reacting-air predictions originates in the significance of internal energy. In a perfect gas, the internal energy is due to rotation and translation kinetic energy, which determines species collision intensity, hence pressure. Within a reacting gas, on the other hand, internal energy also encompasses vibrational and formation energy, hence only a portion of ε contributes to the pressure causing molecular kinetic energy, which corresponds to a reduction in both pressure and pressure increase in comparison to the perfect-gas case.

As ε increases further, the curves tend to approach straight lines, because at completion of the chemical reactions, the equilibrium air begins to behave for a certain range of temperature as a perfect gas of atomic oxygen and nitrogen, corresponding to the first EOS in (6) with $\gamma = \frac{5}{3}$. This pressure distribution remains continuous and smooth.

The kinetic-theory interpretation of pressure as collisional variation of linear momentum [11, 13, 14] explains the variations of the partial derivatives of pressure. Concerning the variation of the constant-density derivative $(\partial p/\partial \varepsilon)_\rho$, as temperature increases the mixture species possess greater kinetic energy, hence this derivative is positive. An increase in temperature with constant pressure, however, leads to a decrease in density, hence fewer particles collide, pressure increases less rapidly and $(\partial p/\partial \varepsilon)_\rho$ decreases as temperature increases. In the presence of chemical reactions, on the other hand, more particles collide hence this derivative is greater than in the perfect-gas case.

For a fixed ε, as temperature increases, an increase in mixture density corresponds to more species involved in collisions, which explains the increase in $(\partial p/\partial \rho)_\varepsilon$ for both the non-reacting and reacting cases. This thermodynamic derivative varies linearly for low temperature, because for a perfect gas, hence from (6), this derivative equals ε, which from (6) increases linearly with temperature. As temperature increases, the reacting-air values of this derivative are greater than those for a perfect-air, because the chemical reactions lead to more colliding species than in the perfect-air case. For both derivatives, a dissociation-favouring decrease in pressure then further reduces the increase in molecular kinetic energy and increases the number of colliding species, which explains the observed respective variations of these derivatives with respect to pressure. As temperature increases further, the chemical dissociations are complete, the mixture becomes a perfect gas of atomic species and the isochors converge to a single straight line. This line corresponds to the derivative of the first expression in (6), but with $\gamma = \frac{5}{3}$, rather than the smaller $\gamma = \frac{7}{5}$, which explains the steeper slope of the atomic-air line versus that for molecular air. Observe that for both these thermodynamic derivatives, the procedure has generated continuous and smooth distributions.

Another clear indication of the significant differences between perfect- and reacting-air behaviour is provided by Figures 6–8. These figures respectively correlate with Figures 3–5 and present the variation of temperature versus internal energy ε and the thermodynamic partial derivatives of temperature versus temperature. For low energies, no chemical reactions occur nor are the vibrational modes fully excited. Consequently, temperature remains independent of pressure and increases linearly with internal energy in this range. This correct trend follows the perfect-gas TE from (6), which shows both independence from pressure and a constant specific heat for the constant slope in the curve. Temperature is a measure of the molecular kinetic-energy mode [11–14]. Hence, further increases in energy, accompanied by chemical reactions, reduce the rise in temperature, in comparison to the perfect-air case, because only part of the internal energy raises molecular kinetic energy, while the rest triggers chemical reactions, and the larger ε the greater the discrepancy between perfect-air and reacting-air predictions.

As the graphs show, the rise in temperature is further retarded by a decrease in pressure, which increases the rate of dissociations and thus further reduces the increase in molecular kinetic energy. For continuing increase of internal-energy, the curves then indicate a diminishing dependence on pressure and concurrent convergence towards a single straight line.

This convergence results from completion of the chemical reactions, hence the equilibrium-air behaves for a certain range of energies as a perfect-gas of atomic oxygen and nitrogen

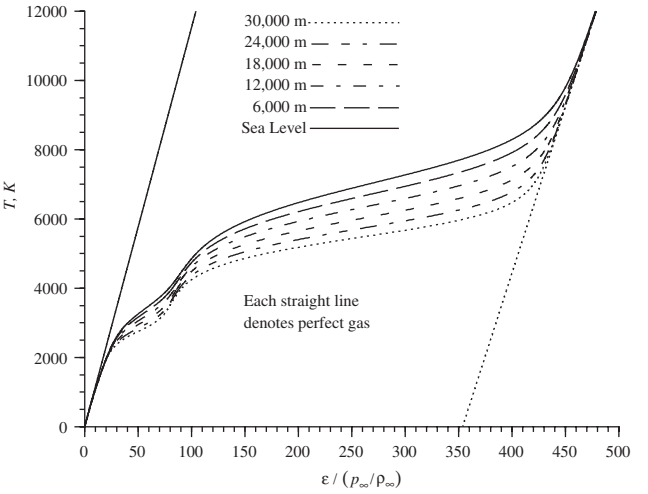

Figure 6. Temperature versus internal energy.

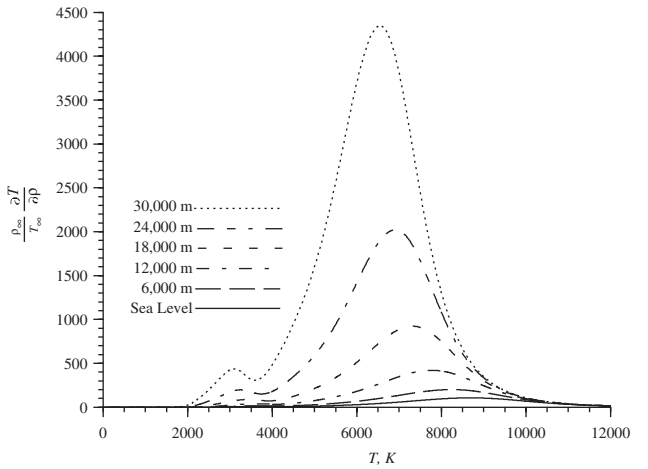

Figure 7. $\rho_\infty/T_\infty(\partial T/\partial\rho)_\varepsilon$ versus temperature.

with pressure-independent constant specific heat, hence the constant slope in the corresponding curve. Overall, the temperature distributions in the figure remain continuous and smooth.

For low temperatures, $(\partial T/\partial\rho)_\varepsilon$ has to vanish, for temperature remains constant for fixed ε, according to the perfect-air TE from (6). As temperature increases, the presence of chemical dissociations induce a strong dependence of T and $(\partial T/\partial\rho)_\varepsilon$ on ρ because an increase in mixture density provides for more atoms in the mixture that become free from molecular bonds and travel faster than molecules because they are less massive. The number and intensity of particle collisions, therefore, increases, impact linear momentum is exchanged more rapidly,

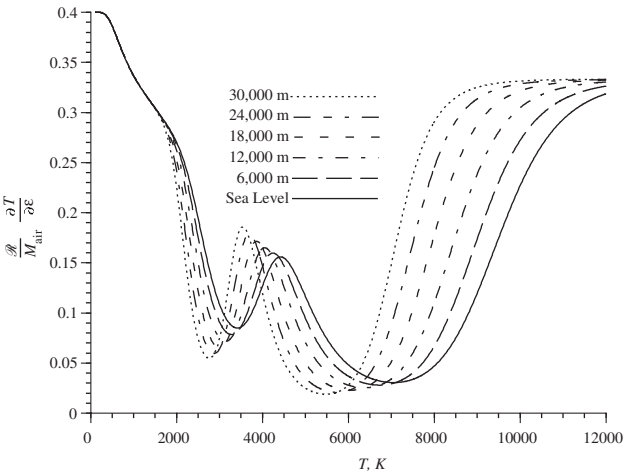

Figure 8. $\mathscr{R}/M_{\text{air}}(\partial T/\partial\varepsilon)_\rho$ versus temperature.

and kinetic energy, hence temperature, increases more swiftly than in the non-reacting case. This effect is accentuated by a dissociation-favouring pressure decrease.

As temperature increases further, however, the dependence of $(\partial T/\partial\rho)_\varepsilon$ on T rapidly decreases because at completion of the chemical reactions, no additional atomic particles emerge within the mixture and internal energy no longer depends on density, but only on temperature. For constant ε, it thus follows that $(\partial T/\partial\rho)_\varepsilon \simeq 0$, in these conditions. The variation of $(\partial T/\partial\varepsilon)_\rho$ versus T directly correlates with the variation of T versus ε and mole fractions versus T. Even before chemical dissociations begin, this derivative is seen to decrease, as determined by the non-linear increase of the vibrational energy, which equals kinetic energy at equilibrium. Therefore, temperature, a measure of one mode of molecular energy among the translational, rotational and vibrational modes, increases less rapidly than ε, the sum of all the molecular energy modes. As the chemical reactions progress, they require increasing amounts of energy that will not be present as kinetic energy, hence $(\partial T/\partial\varepsilon)_\rho$ decreases further. When the peak in nitric oxide mass fraction is reached, an increase in internal energy contributes to a proportional increase in molecular kinetic energy, which explains the increase in $(\partial T/\partial\varepsilon)_\rho$ until a state where a further increase in temperature initiates the dissociation of molecular nitrogen. This dissociation will then require increasing amounts of energy that will not be present as kinetic energy, hence $(\partial T/\partial\varepsilon)_\rho$ begins to decrease again. As the chemical dissociations near completion, an increase in ε induces a proportional increase in molecular kinetic energy, which explains the renewed increase in $(\partial T/\partial\varepsilon)_\rho$. A thermodynamic state is then reached where the reactions are complete, the mixture begins to behave as a perfect air, within an appropriate range of T, and thus $(\partial T/\partial\varepsilon)_\rho$ becomes equal to a constant, corresponding to the inverse of a constant specific-heat. It is important to observe that for both derivatives, the procedure generated smooth results.

Figures 9 and 10 present the variations of the specific heats c_v and c_p versus temperature.

These variations directly correlate with the variation of $(\partial T/\partial\varepsilon)_\rho$ and with each other, following (130). At low temperature, the mixture behaves as a perfect gas of molecular oxygen and nitrogen. From (41)–(42) and (132), therefore, $c_v/(\mathscr{R}/M_{\text{air}})$ and $c_p/(\mathscr{R}/M_{\text{air}})$

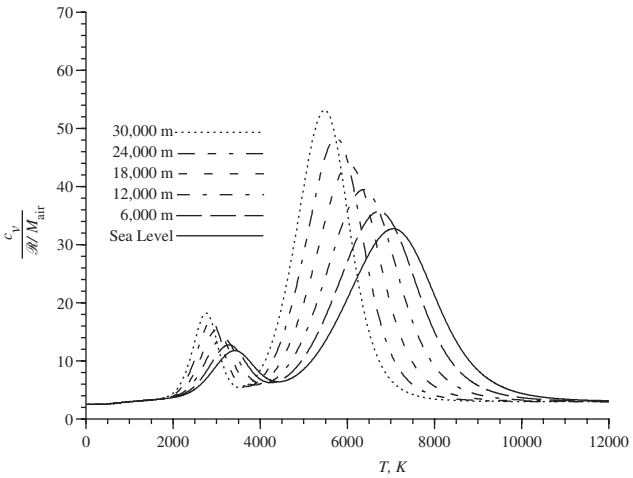

Figure 9. Specific Heat c_v versus temperature.

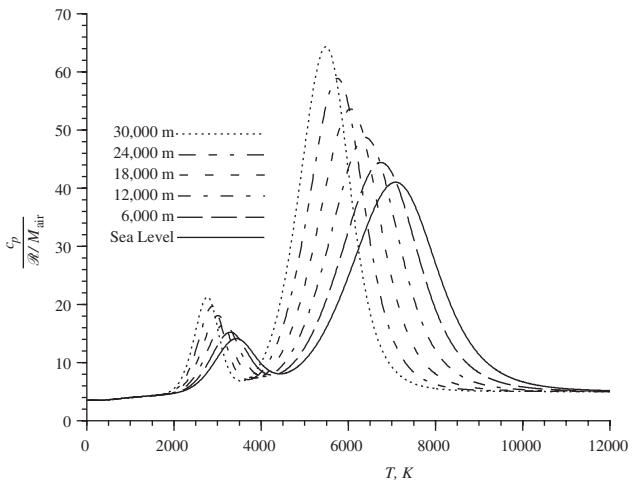

Figure 10. Specific Heat c_p versus temperature.

approach their respective perfect-gas magnitudes of $\frac{5}{2}$ and $\frac{7}{2}$. Before any chemical reactions, pressure does not influence c_v and c_p, but as temperature increases, c_v and c_p rise above corresponding perfect-gas magnitudes because the internal energy experiences an increase in both kinetic energy, contributing perfect-gas magnitudes for these specific heats, and vibrational energy. With the onset of chemical reactions, the rate of change of Y_3 initially increases with temperature and internal energy and enthalpy rapidly increase through NO formation enthalpy, which leads to the observed rapid rise in c_v and c_p. When the NO mass fraction decreases with temperature, so does the corresponding formation-enthalpy contribution to internal energy and enthalpy. Consequently both c_v and c_p decrease, but remain greater than

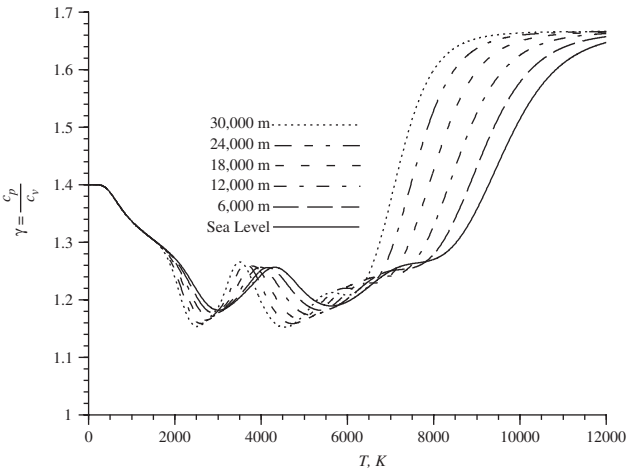

Figure 11. Specific heat ratio γ versus temperature.

perfect gas levels owing to vibrational energy modes and the increasing contribution of atomic-oxygen formation enthalpy. As temperature increases further, the mass and mole fraction of N rapidly rise, hence the internal energy significantly increases due to the increasing contribution from the formation enthalpy of N. A decrease in pressure favours the mixture chemical reactions and it thereby accentuates the effects of NO and N formation-enthalpy contributions to internal energy, which intensifies the rises in c_v and c_p. For $T \leqslant 9000\,\mathrm{K}$, hence in the virtual absence of electrons and ionic species, the distribution of $c_v/(\mathscr{R}/M_{\mathrm{air}})$ agrees with the one reported in Reference [14]. For higher temperatures, the mass fraction of N increases less rapidly until it reaches a constant plateau. Accordingly, c_v and c_p begin to decrease and a further temperature rise merely increases atomic kinetic energy. The mixture thus behaves as a non-reacting gas that consists of atomic oxygen and nitrogen. The atomic mass of this mixture equals half of M_{air}, and from (41)–(42) and (132), $c_v/(\mathscr{R}/M_{\mathrm{air}})$ and $c_p/(\mathscr{R}/M_{\mathrm{air}})$ approach their respective perfect-gas magnitudes of 3 and 5.

Figures 11 and 12 show the variation of specific heat ratio γ and non-dimensional sound speed squared $c^2/(p/\rho)$. Without any chemical reactions or vibrational-energy effects, both γ and $c^2/(p/\rho)$ equal the molecular perfect-gas magnitude of $\frac{7}{5}$. From the first expression in (131), γ equals the product of the derivative of enthalpy with respect to temperature and the derivative of temperature with respect to internal energy. The variation of γ, therefore, directly correlates with the variation of $(\partial T/\partial \varepsilon)_\rho$, portrayed in Figure 8. In the absence of chemical reactions, all terms beyond γRT vanish in expression (137) for the square of the speed of sound. In these conditions, therefore, γ and $c^2/(p/\rho) = c^2/(RT)$ equal each other, as Figures 11 and 12 indicate. When the mixture chemical reactions take place, expression (137) shows that $c^2/(p/\rho)$ no longer coincides with γ, as the charts indicate. For $T \leqslant 9000\,\mathrm{K}$, hence in the virtual absence of electrons and ionic species, the distribution of $c^2/(p/\rho)$ agrees with the one reported in Reference [14].

When the reactions are completed, γ and $c^2/(p/\rho)$ coincide with each other again and approach the perfect-gas magnitude of $\frac{5}{3}$, following expressions from (41)–(42) and (132).

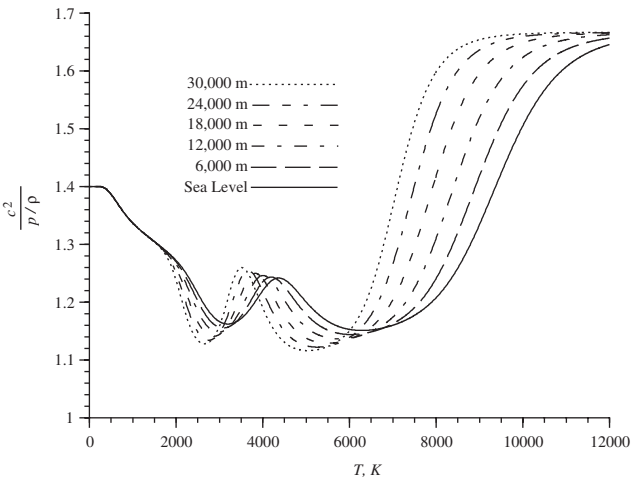

Figure 12. Sound speed squared versus temperature.

13. CONCLUDING REMARKS

The procedure detailed in this paper directly generates pressure, and temperature, as well as their thermodynamic and jacobian partial derivatives, mass and mole fractions, molecular mass, specific heats and speed of sound for a five-species neutral equilibrium air. Owing to the exact, physically meaningful solution of the mass-fraction and mass-action equations, this procedure algebraically reduces the six-equation chemical-equilibrium thermodynamic system and explicitly expresses four variables in terms of nitric-oxide mass fraction and temperature. These two variables are then numerically determined by solving the internal-energy and nitric-oxide mass-action equations through a Newton's method solution, which is observed to converge rapidly in two to three iterations. The procedure then exactly determines the partial derivatives of pressure, temperature and mass fractions analytically.

All of the computational results over a temperature range of more than 10 000 K and pressure range corresponding to an increase in altitude of 30 000 m, about 98 000 ft, above sea level, remain physically meaningful. Independently published results are available for mole fractions, constant-volume specific-heat and speed of sound and the distributions of these variables predicted by the procedure agree with these independent results. The thermodynamic properties so generated, including the critical thermodynamic partial derivatives of pressure and temperature are then observed to remain continuous and smooth. These results, therefore, support the procedure as an attractive alternative both to generate the thermodynamic properties of electrically neutral chemically reacting equilibrium air and to incorporate these properties directly and efficiently within Euler and Navier–Stokes CFD algorithms.

REFERENCES

1. Tannehill JC, Mugge PH. Improved curve fits for the thermodynamic properties of equilibrium air suitable for numerical computation using time-dependent or shock-capturing methods. *NASA CR-2470*, 1974.

2. Liou MS, van Leer B, Shuen JS. Splitting of inviscid fluxes for real gases. *Journal of Computational Physics* 1990; **87**:1–24.
3. Janicka J, Peters N. Asymptotic evaluation of mean NO production rate in turbulent diffusion flames. *Combustion Science and Technology* 1980; **22**:93.
4. Prabhu RK, Stewart JR, Thareja RR. A Navier–Stokes solver for high speed equilibrium flows and application to blunt bodies. *AIAA 89-0668*, 27th Aerospace Sciences Meeting, Reno, NV, 1989.
5. Yee HC, Klopfer GH, Montagne JL. High resolution shock-capturing schemes for inviscid and viscous hypersonic flows. *Journal of Computational Physics* 1990; **88**:31–61.
6. Park C. On convergence of computation of chemically reacting flows. Technical Paper, *AIAA 85-0247*, 23rd Aerospace Sciences Meeting, Reno, NV, 1985.
7. Park C, Yoon S. A fully-coupled implicit method for thermo-chemical non-equilibrium air at sub-orbital flight speeds. Technical Paper, *AIAA 89-1974*, 9th Computational Fluid Dynamics Conference, Buffalo, New York, 1989.
8. Desideri J-A, Glinsky N, Hettena E. Hypersonic reacting flow computations. *Computers and Fluids* 1990; **18**(2):151–182.
9. Maas U, Pope S. Simplifying chemical kinetics: intrinsic low dimensional manifolds in composition space. *Combustion Flame* 1992; **88**:239.
10. Pope S. Computationally efficient implementation of combustion chemistry using in situ adaptive tabulation. *Combustion Theory and Modelling* 1997; **1**:85.
11. Greiner W, Neise L, Stöcker H. *Thermodynamics and Statistical Mechanics*. Springer: New York, 1997.
12. Rasmussen M. *Hypersonic Flow*. John Wiley: New York, 1994.
13. Vincenti WG, Kruger CH. *Introduction to Physical Gas Dynamics*. Wiley: New York, 1965.
14. Anderson Jr. JD. *Hypersonic and High Temperature Gas Dynamics*. Mc Graw-Hill: New York, 1989.
15. Gnoffo PA, Gupta RN, Shinn JL. Conservation equations and physical models for hypersonic air flows in thermal and chemical nonequilibrium. *NASA Technical Paper 2868*, 1989.
16. Emsley J. *The Elements*. Oxford University Press: New York, 1998.
17. Gupta RN, Yos JM, Thompson RA, Lee K-P. A review of reaction rates and thermodynamic and transport properties for an 11-species air model for chemical and thermal nonequilibrium calculations to 30 000K. *NASA Reference Publication 1232*, 1990.
18. Meintjes K, Morgan AP. Element variables and the solution of complex chemical equilibrium problems. *Combustion Science and Technology* 1989; **68**:35–48.
19. Iannelli J. A CFD euler solver from a physical acoustics—convection flux Jacobian decomposition. *International Journal for Numerical Methods in Fluids* 1999; **31**:821–860.

